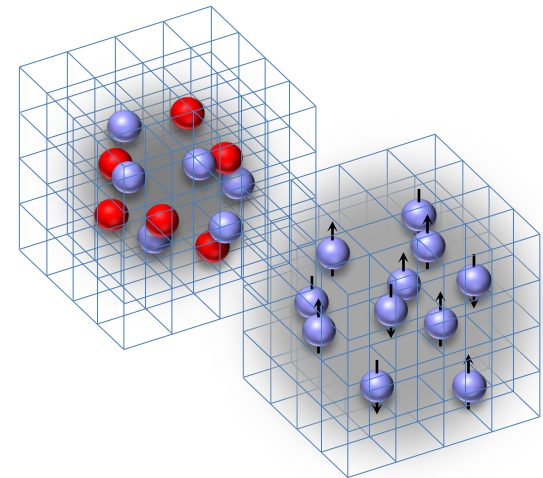


# *Ab initio* nuclear structure theory and implications for relativistic heavy-ion collisions

Dean Lee  
Facility for Rare Isotope Beams  
Michigan State University  
Nuclear Lattice EFT Collaboration

Physics Colloquium and  
STAR Collaboration Meeting  
Brookhaven National Laboratory  
March 22, 2024



## Outline

*Ab initio* methods

Lattice effective field theory

Essential elements for nuclear binding

Emergent geometry and duality of  $^{12}\text{C}$

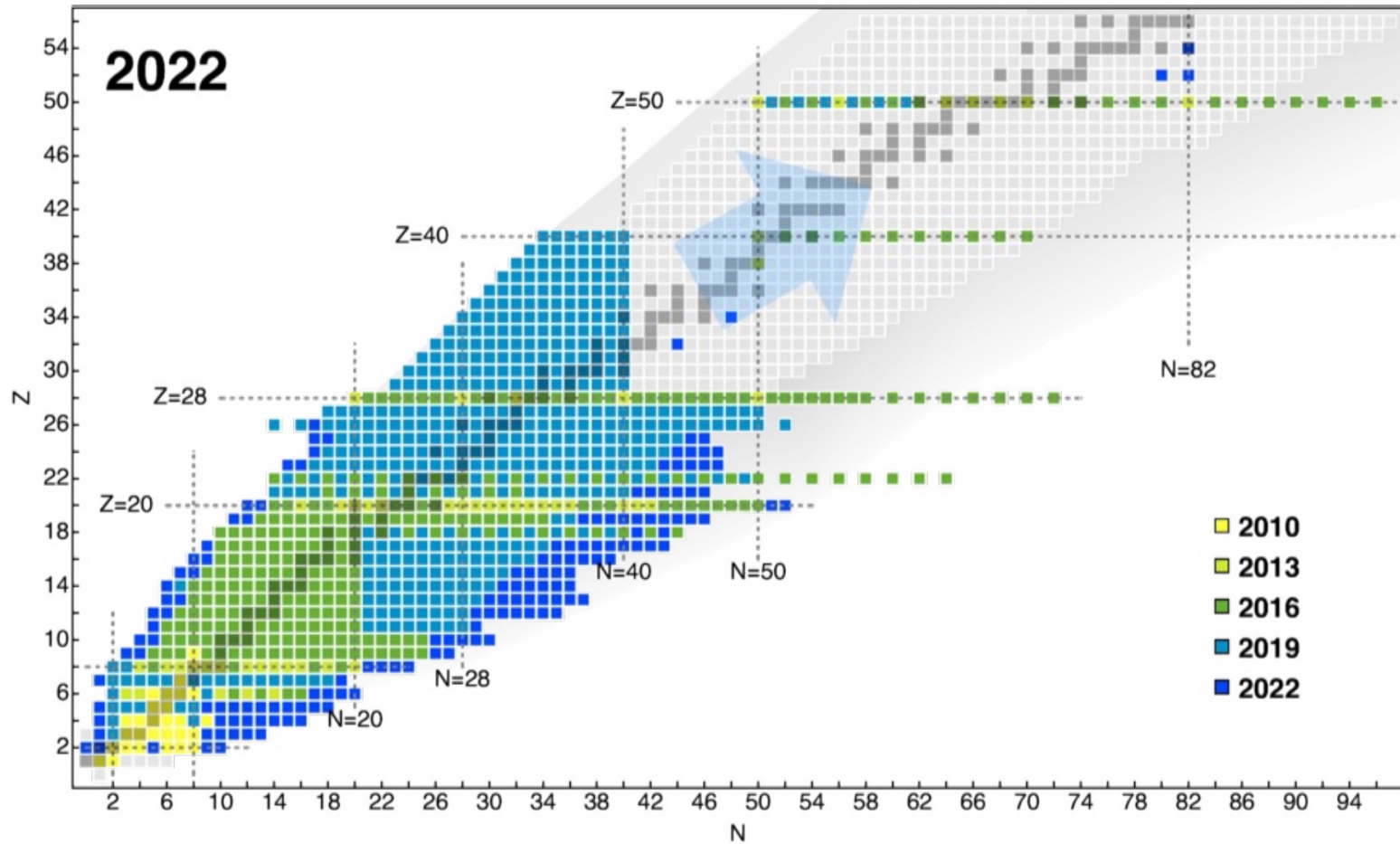
Wave function matching

$^{16}\text{O}^{16}\text{O}$  collisions at RHIC and LHC energies

$^{16}\text{O}^{16}\text{O}$  versus  $^{20}\text{Ne}^{20}\text{Ne}$  collisions

Outlook

## Ab initio methods



adapted from Hergert, Front. Phys. 8, 379 (2020)

# Many-Body Perturbation Theory

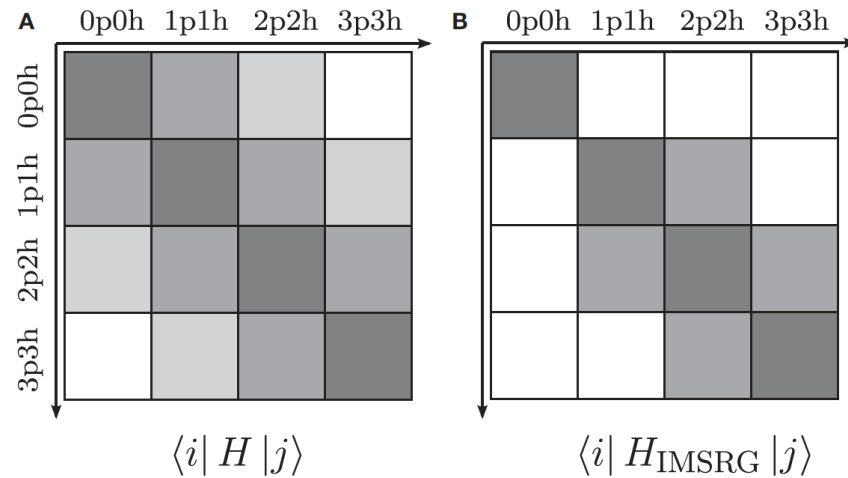
Roth et al., Phys. Lett. B683, 272 (2010); Tichai et al., Phys. B756, 283 (2016)

$$|\Psi\rangle = |\Phi\rangle + \sum_{n=1}^{\infty} \left( \frac{1}{H_0 - E^{(0)}} H_I \right)^n |\Phi\rangle$$

$$E = E^{(0)} + \langle \Phi | \sum_{n=1}^{\infty} H_I \left( \frac{1}{H_0 - E^{(0)}} H_I \right)^n | \Phi \rangle$$

## In-Medium Similarity Renormalization Group

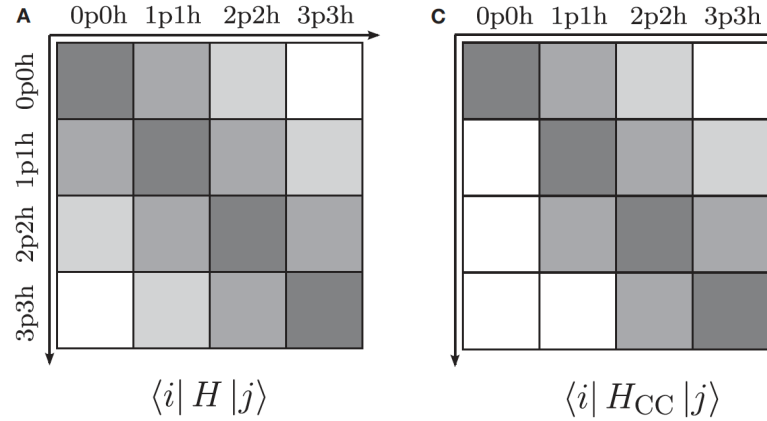
Hergert et al., Phys. Rev. 621, 165 (2016); Stroberg et al., Phys. Rev. Lett. 118, 032502 (2017)



Hergert, Front. Phys. 8, 379 (2020)

## Coupled Cluster Methods

Hagen et al., Rept. Prog. Phys. 77, 096302 (2014); Duguet et al., Phys. Rev. C 91, 064320 (2015)



## Self-Consistent Green's Functions

Dickhoff et al., Prog. Part. Nucl. Phys. 52, 377 (2004), Soma et al. Phys. Rev. C 101, 014318 (2020)

$$g_{pq\dots rs} = \langle \Psi_0^A | T [a_p(t_p) a_q(t_q) \cdots a_s^\dagger(t_s) a_r^\dagger(t_r)] | \Psi_0^A \rangle$$

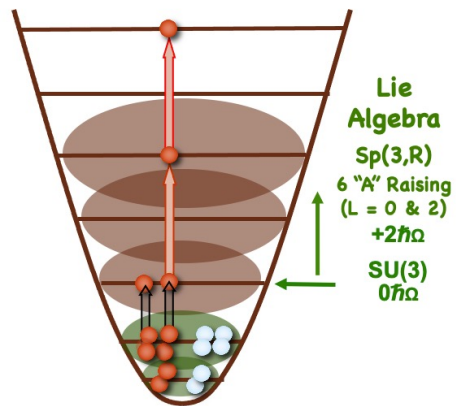
## No-Core Configuration Interaction

Barrett et al., Prog. Part. Nucl. Phys. 69, 131 (2013); Navratil et al., Phys. Scripta. 91 053002, (2016)

$$|\Psi\rangle = |\Psi\rangle_{\text{core}} \otimes |\Psi\rangle_{\text{valence}} \rightarrow |\Psi\rangle_{\text{all valence}}$$

## Symmetry-Adapted No-Core Configuration Interaction

Launey et al., Prog. Part. Nucl. Phys. 89, 101 (2016); Dytrych et al. Phys. Rev. Lett. 124, 042501 (2020)



## Projected Variational Methods

Otsuka et al., Prog. Part. Nucl. Phys. 47, 319 (2001); Shimizu, Phys. Scripta. 92, 063001 (2017)

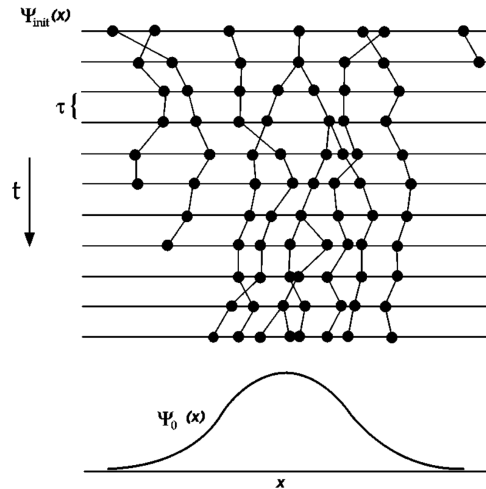
Frosini et al., Eur. Phys. J A 58, 63 (2022), Frosini et al., Eur. Phys. J A 58, 64 (2022)

$$|\Phi_i(J, M, \pi)\rangle = \sum_{K=-J}^J g_K P_{M,K}^J P^\pi |\phi_i\rangle$$

$$|\Psi(J, M, \pi)\rangle = \sum_{i=1}^{N_{\text{basis}}} f_i |\Phi_i(J, M, \pi)\rangle$$

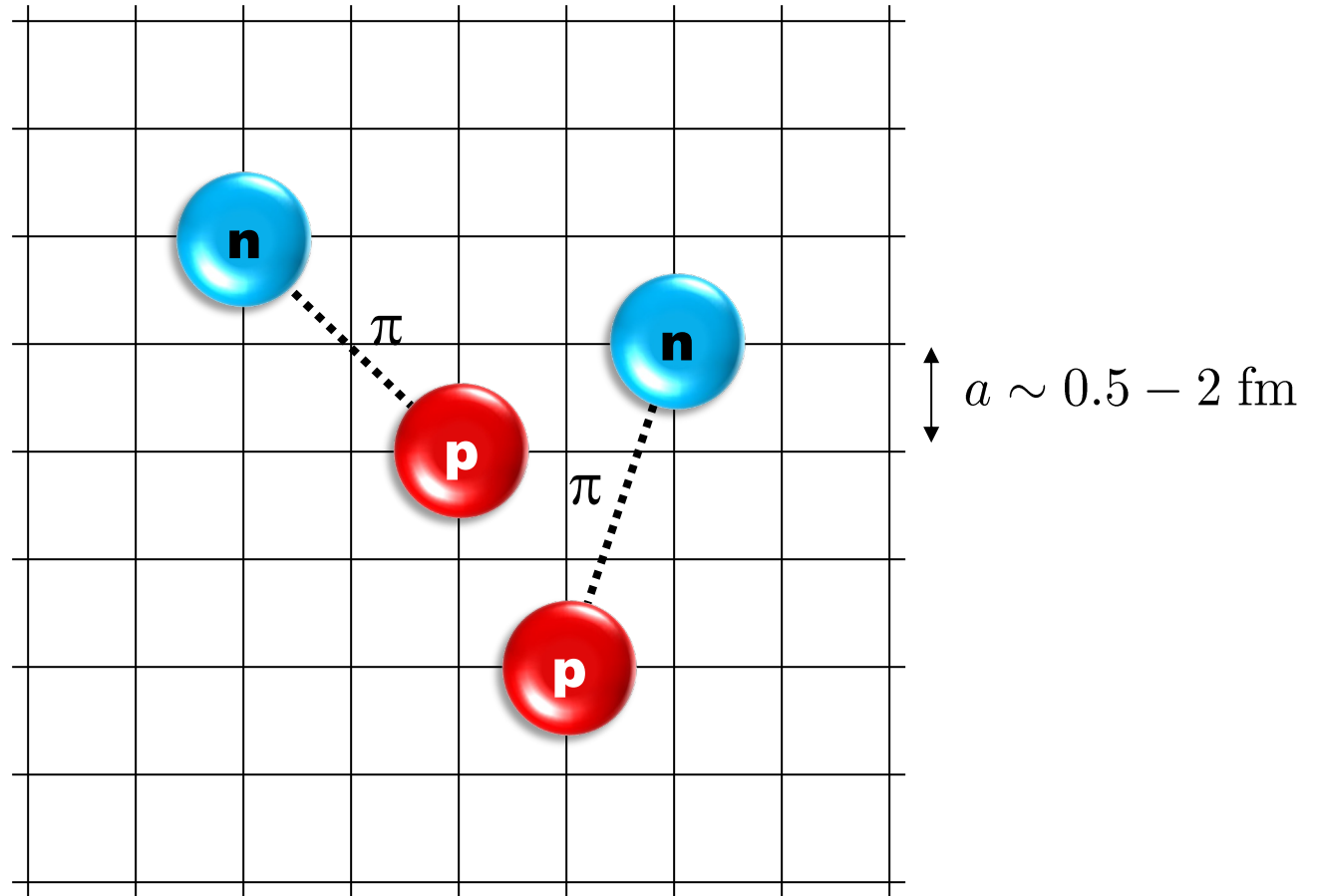
## Quantum Monte Carlo

Carlson et al., Rev. Mod. Phys. 87, 1067 (2015); Gandolfi et al, Front. Phys. 8, 117 (2020)



[Foulkes et al., Rev. Mod. Phys. 73, 1 (2001)]

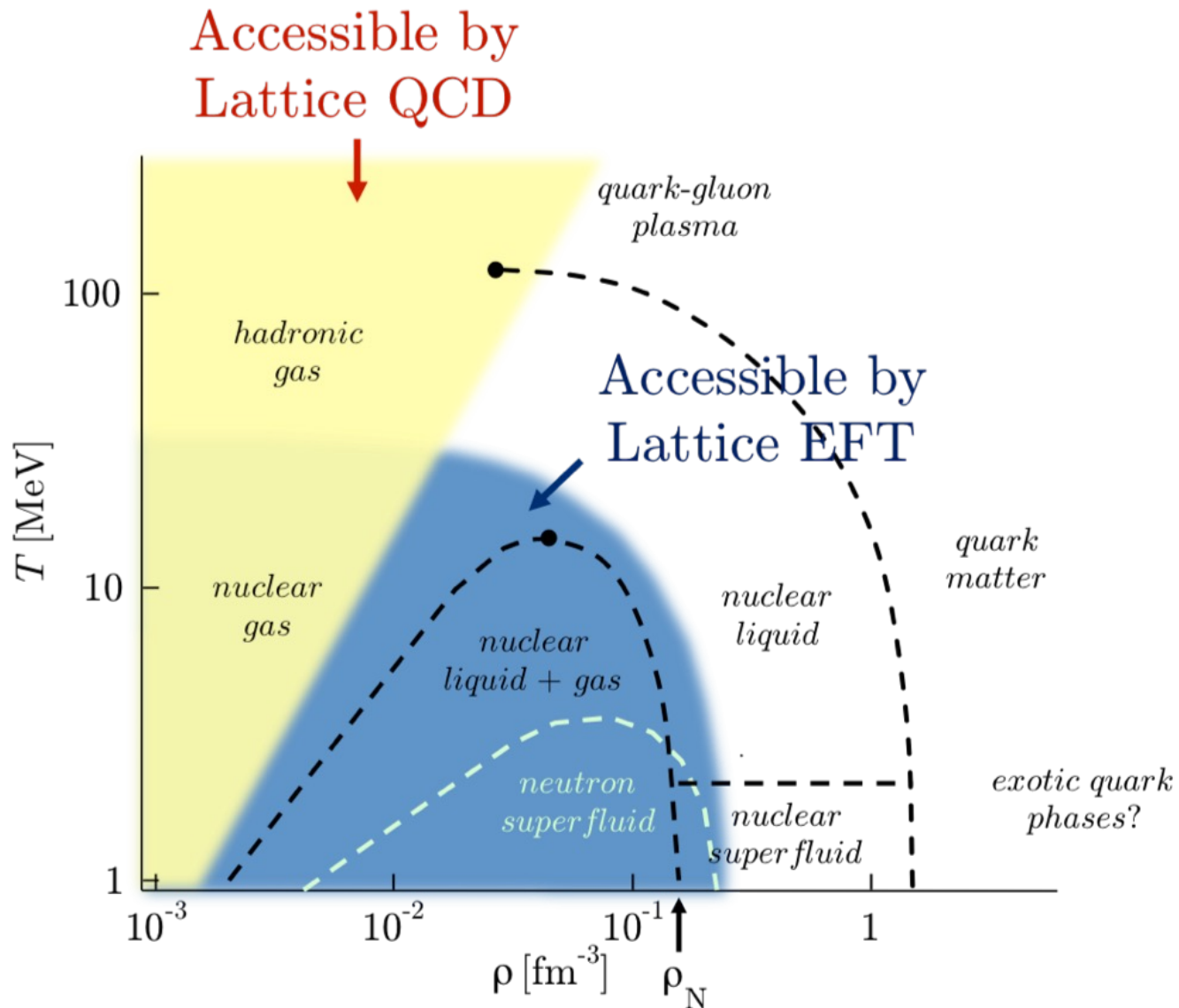
## Lattice effective field theory



D.L, Prog. Part. Nucl. Phys. 63 117-154 (2009)

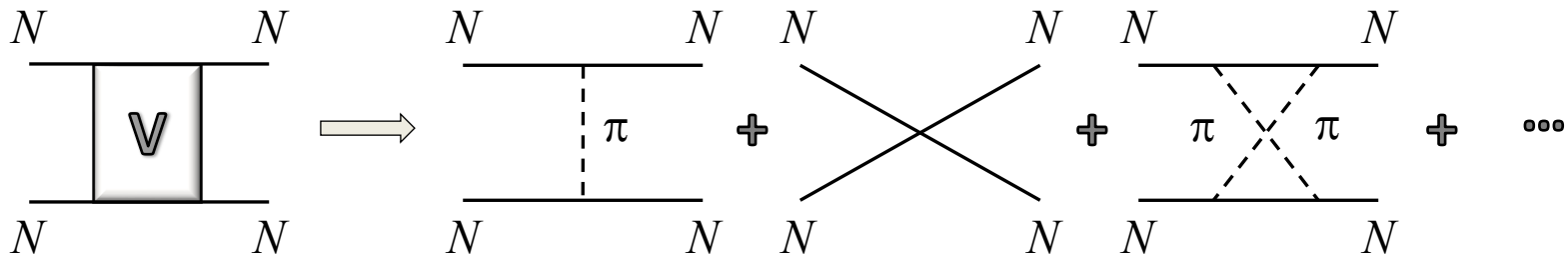
Lähde, Meißner, Nuclear Lattice Effective Field Theory (2019), Springer





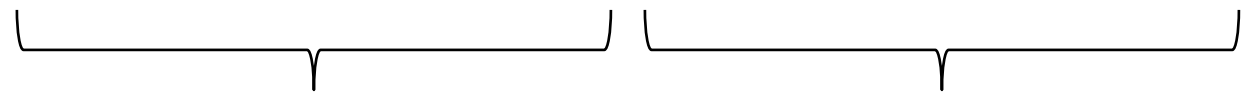
## Chiral effective field theory

Construct the effective potential order by order



$V^{\text{OPEP}}$  Contact interactions

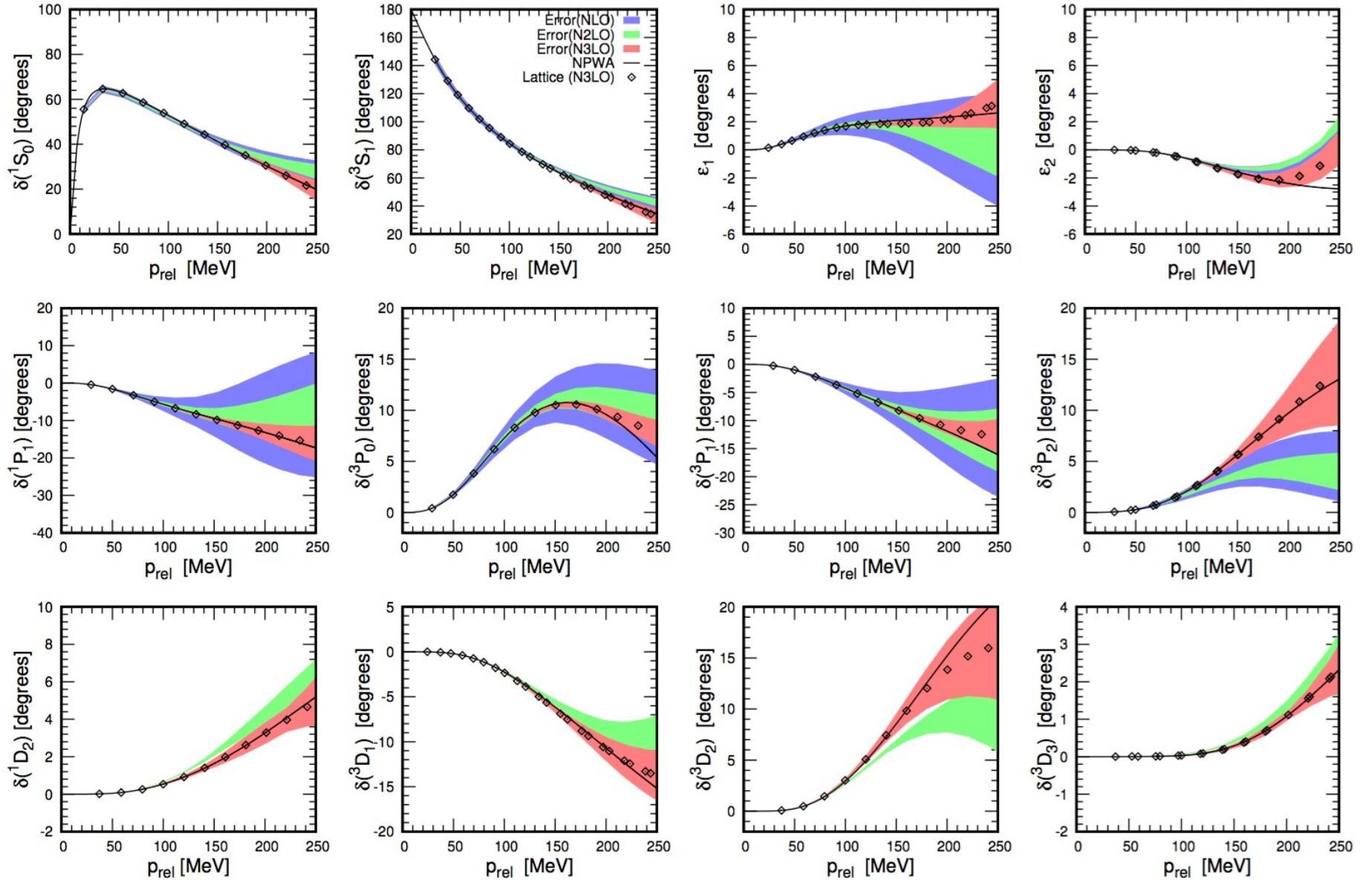
$V^{\text{TPEP}}$



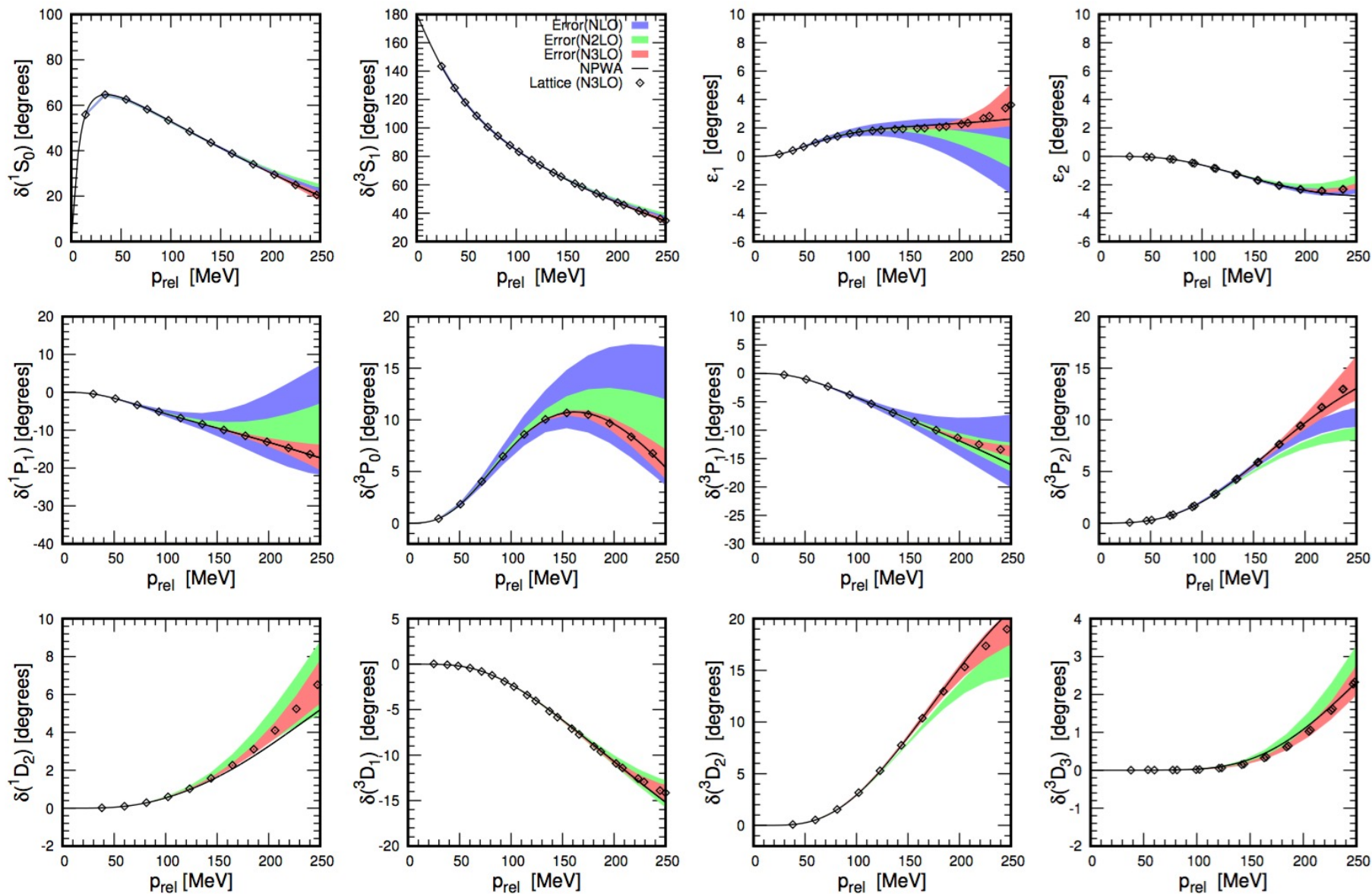
Leading order (LO)

Next-to-leading order (NLO)

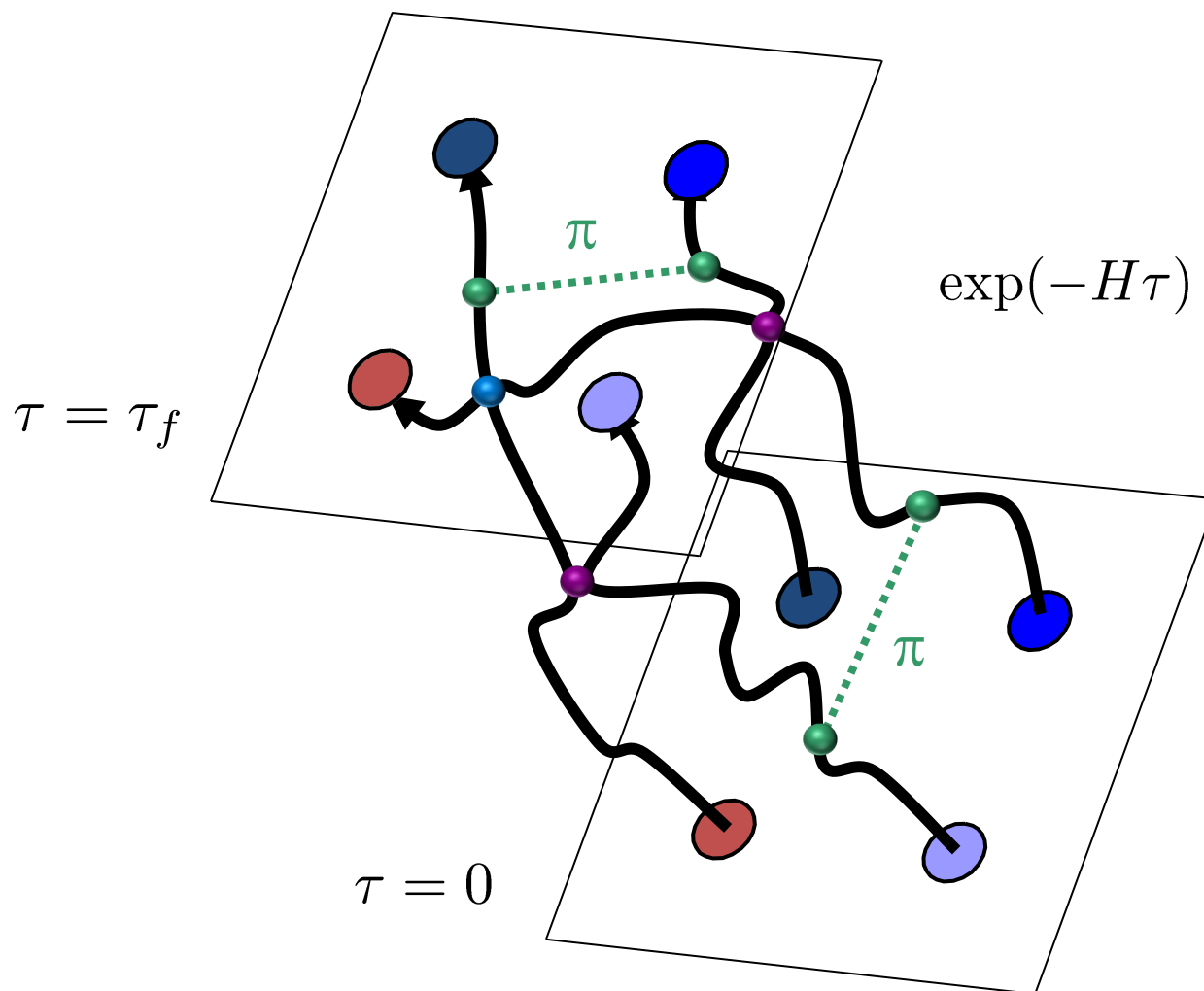
$$a = 1.315 \text{ fm}$$



$$a = 0.987 \text{ fm}$$



## Euclidean time projection



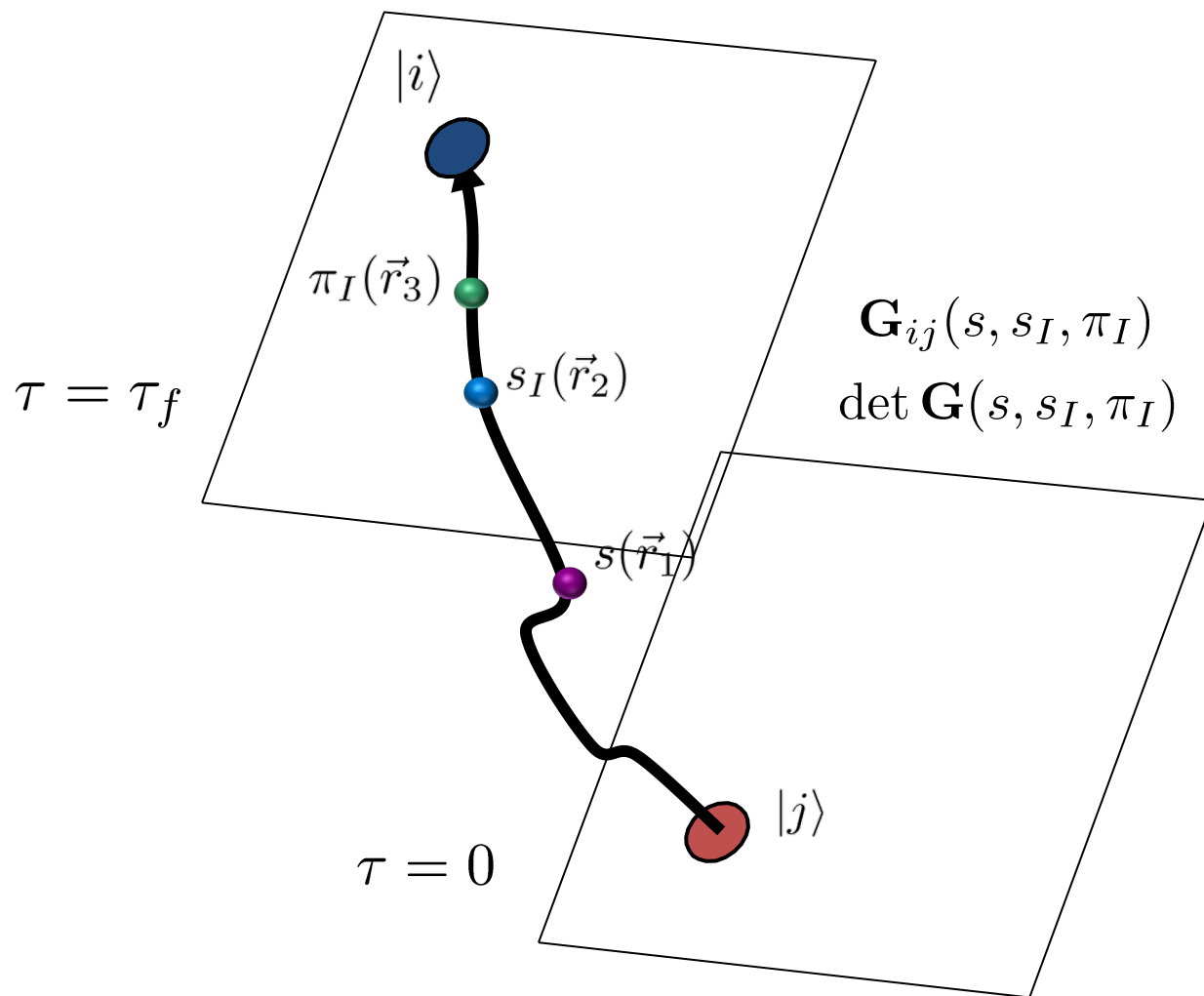
## Auxiliary field method

We can write exponentials of the interaction using a Gaussian integral identity

$$\exp \left[ -\frac{C}{2} (N^\dagger N)^2 \right] \quad \text{X} \quad (N^\dagger N)^2$$

$$= \sqrt{\frac{1}{2\pi}} \int_{-\infty}^{\infty} ds \exp \left[ -\frac{1}{2} s^2 + \sqrt{-C} s (N^\dagger N) \right] \quad \text{Y} \quad s N^\dagger N$$

We remove the interaction between nucleons and replace it with the interactions of each nucleon with a background field.



## Essential elements for nuclear binding

What is the minimal nuclear interaction that can reproduce the ground state properties of light nuclei, medium-mass nuclei, and neutron matter simultaneously with no more than a few percent error in the energies and charge radii?

We construct an interaction with only four parameters.

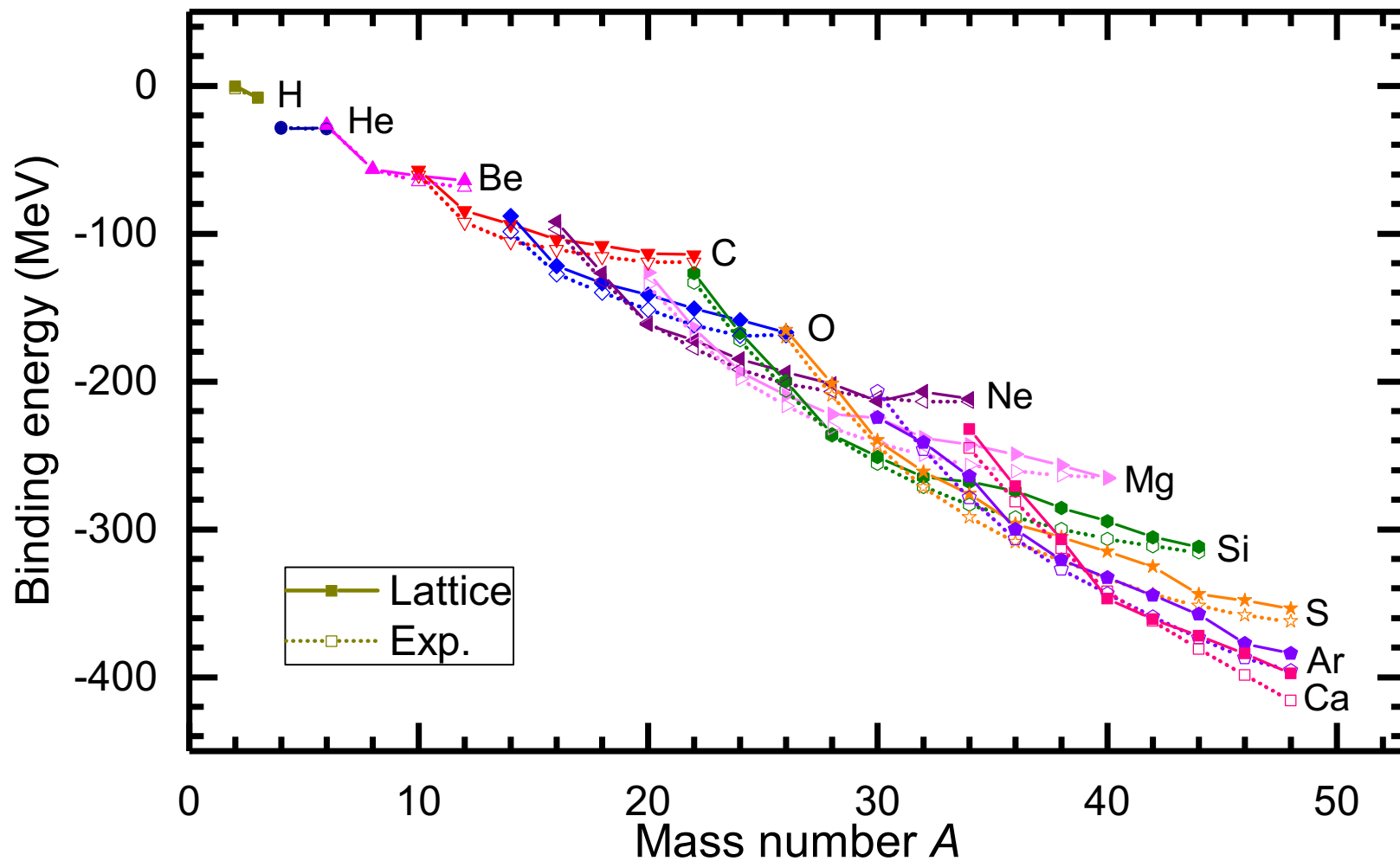
1. Strength of the two-nucleon  $S$ -wave interaction
2. Range of the two-nucleon  $S$ -wave interaction
3. Strength of three-nucleon contact interaction

fit to  
 $A = 2, 3$  systems

4. Range of the local part of the two-nucleon interaction

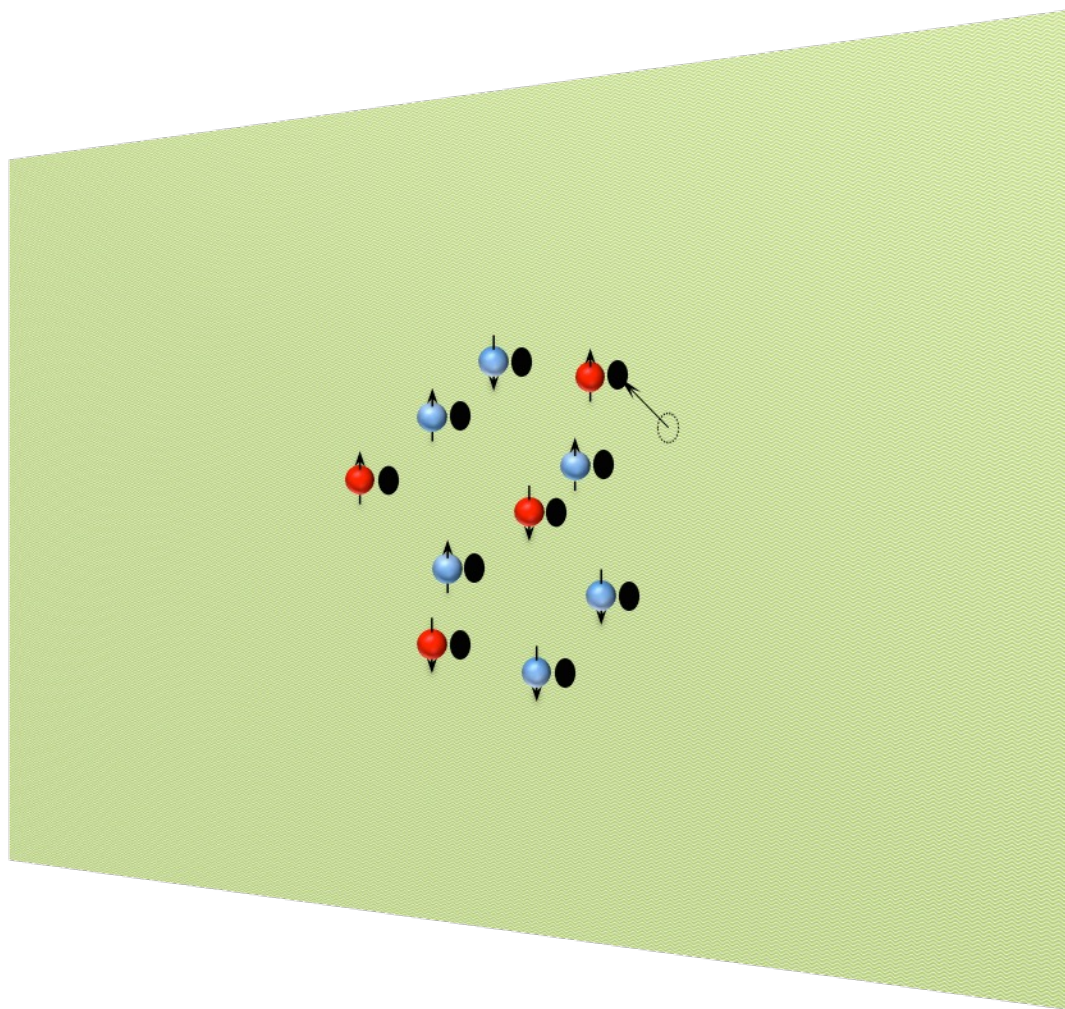
fit to  $A > 3$





	$B$	Exp.	$R_{\text{ch}}$	Exp.
$^3\text{H}$	8.48(2)(0)	8.48	1.90(1)(1)	1.76
$^3\text{He}$	7.75(2)(0)	7.72	1.99(1)(1)	1.97
$^4\text{He}$	28.89(1)(1)	28.3	1.72(1)(3)	1.68
$^{16}\text{O}$	121.9(1)(3)	127.6	2.74(1)(1)	2.70
$^{20}\text{Ne}$	161.6(1)(1)	160.6	2.95(1)(1)	3.01
$^{24}\text{Mg}$	193.5(02)(17)	198.3	3.13(1)(2)	3.06
$^{28}\text{Si}$	235.8(04)(17)	236.5	3.26(1)(1)	3.12
$^{40}\text{Ca}$	346.8(6)(5)	342.1	3.42(1)(3)	3.48

## Pinhole algorithm



## Seeing Structure with Pinholes

Consider the density operator for nucleon with spin  $i$  and isospin  $j$

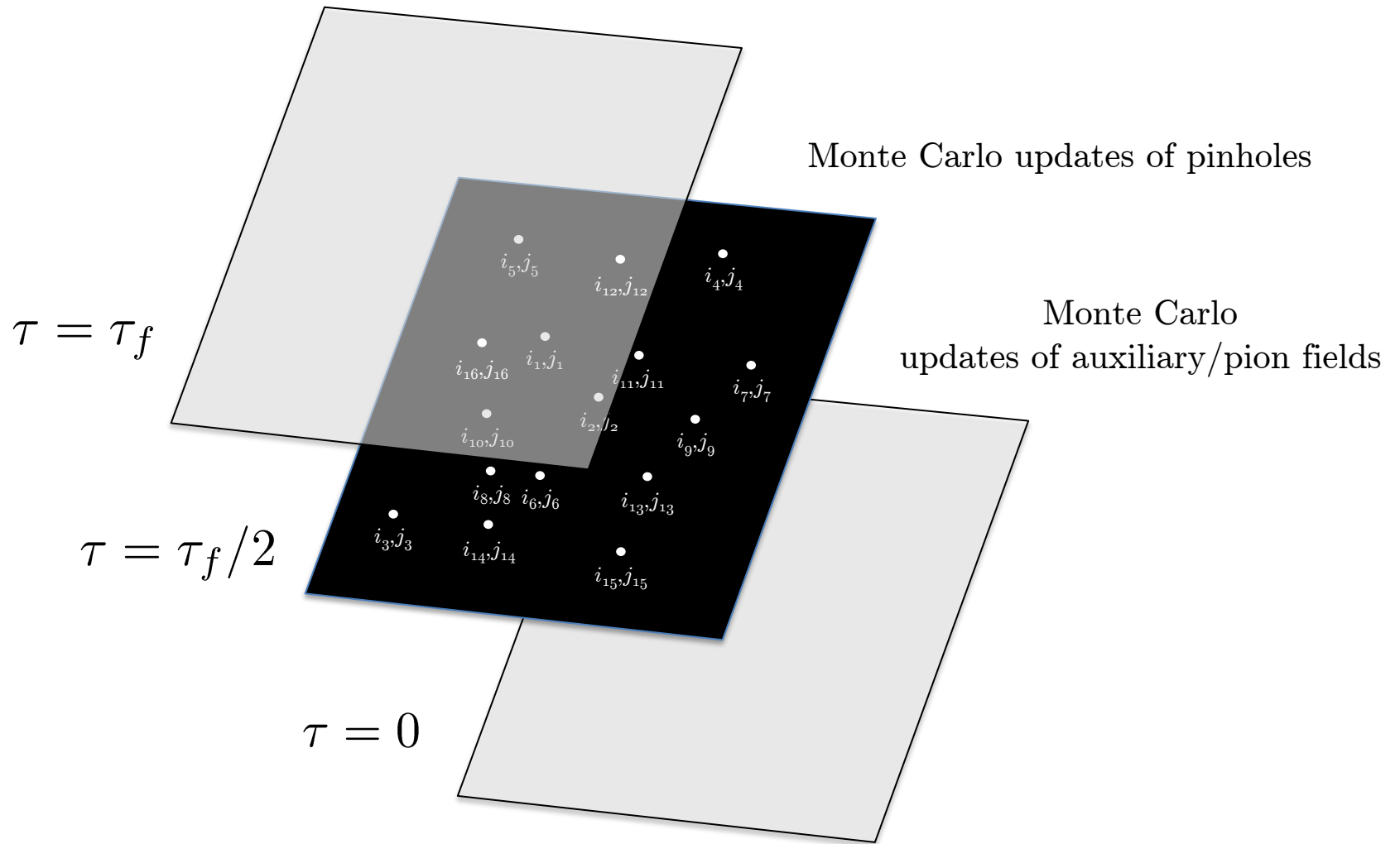
$$\rho_{i,j}(\mathbf{n}) = a_{i,j}^\dagger(\mathbf{n})a_{i,j}(\mathbf{n})$$

We construct the normal-ordered  $A$ -body density operator

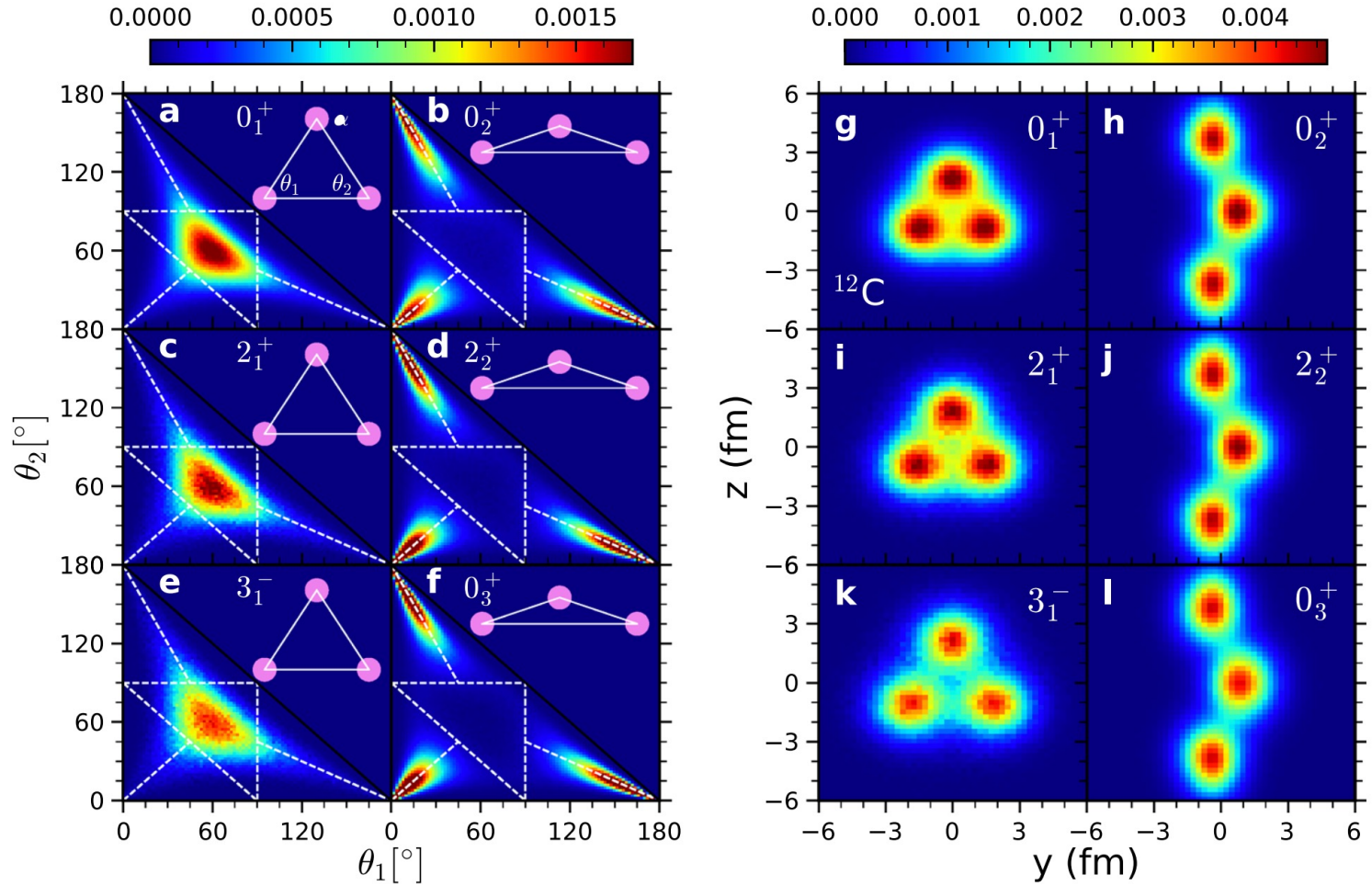
$$\rho_{i_1,j_1,\dots,i_A,j_A}(\mathbf{n}_1,\dots,\mathbf{n}_A) = : \rho_{i_1,j_1}(\mathbf{n}_1) \cdots \rho_{i_A,j_A}(\mathbf{n}_A) :$$

In the simulations we do Monte Carlo sampling of the amplitude

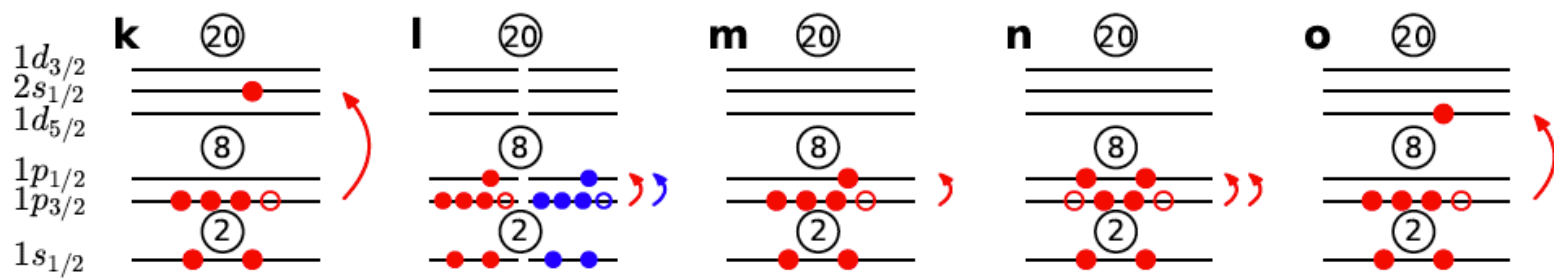
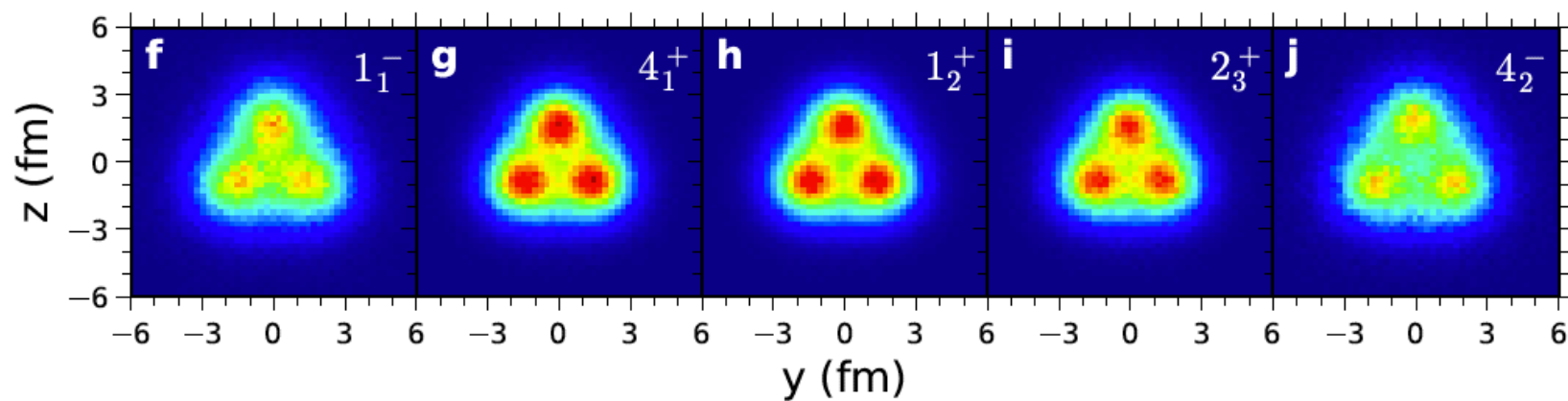
$$A_{i_1,j_1,\dots,i_A,j_A}(\mathbf{n}_1,\dots,\mathbf{n}_A,t) = \langle \Psi_I | e^{-Ht/2} \rho_{i_1,j_1,\dots,i_A,j_A}(\mathbf{n}_1,\dots,\mathbf{n}_A) e^{-Ht/2} | \Psi_I \rangle$$

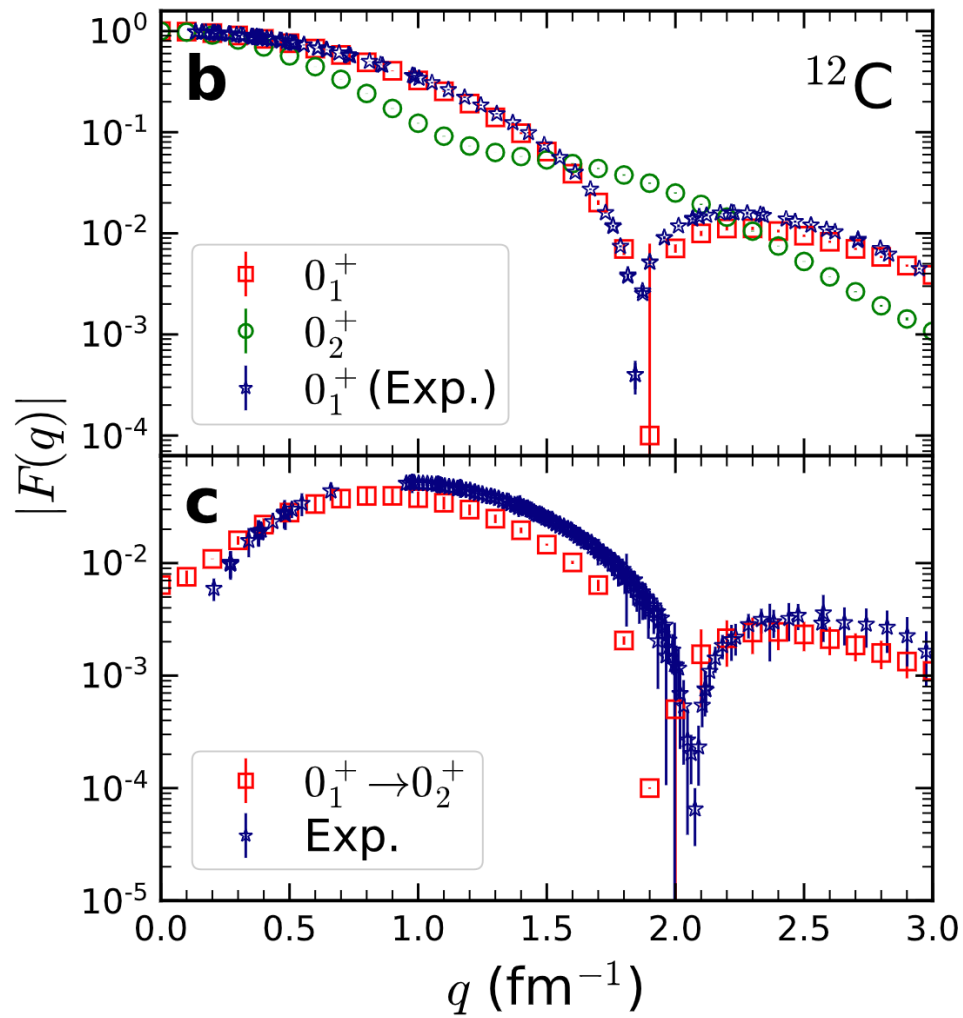


# Emergent geometry and duality of $^{12}\text{C}$



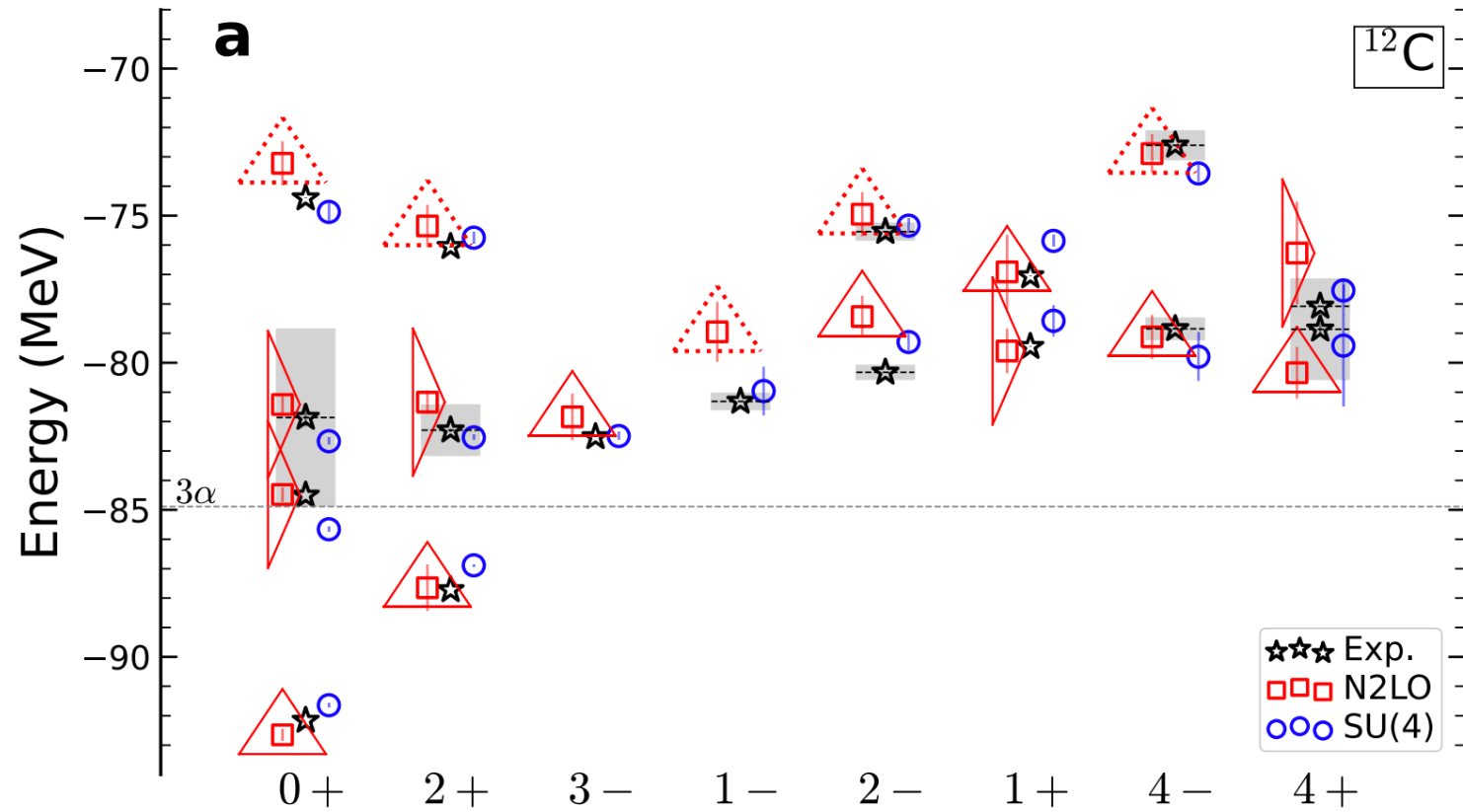
Shen, Elhatisari, Lähde, D.L., Lu, Meißner, Nature Commun. 14, 2777 (2023)





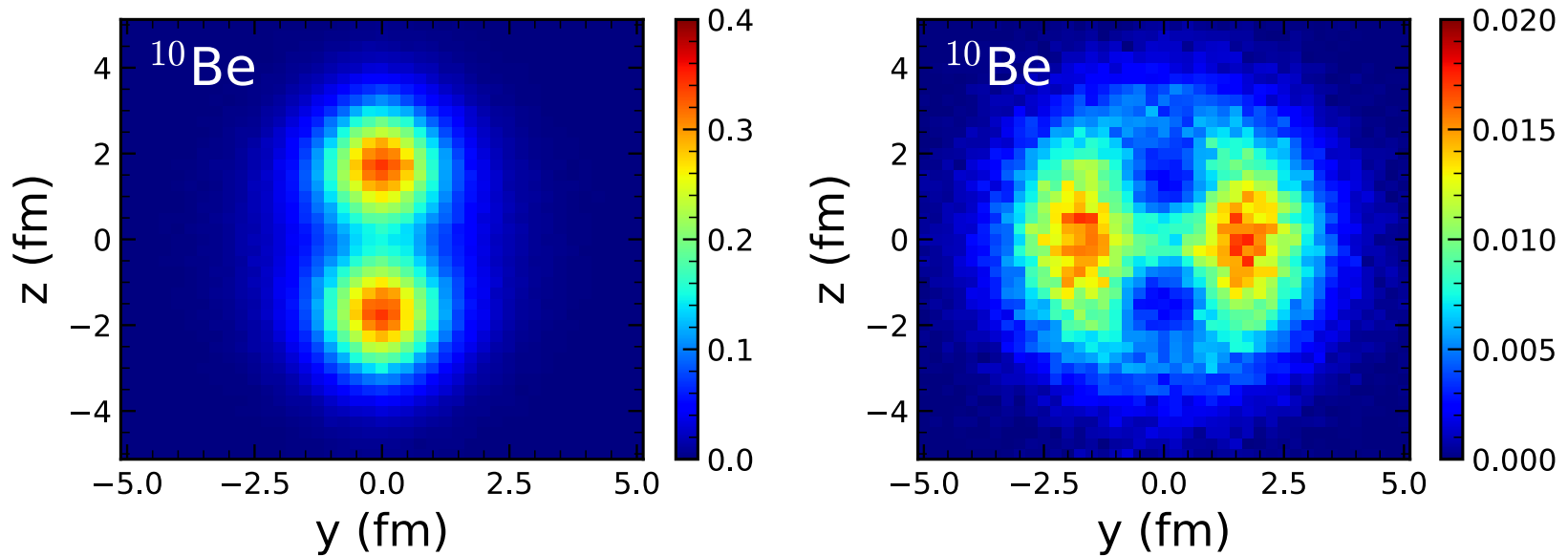
Shen, Elhatisari, Lähde, D.L., Lu, Meißner, Nature Commun. 14, 2777 (2023)





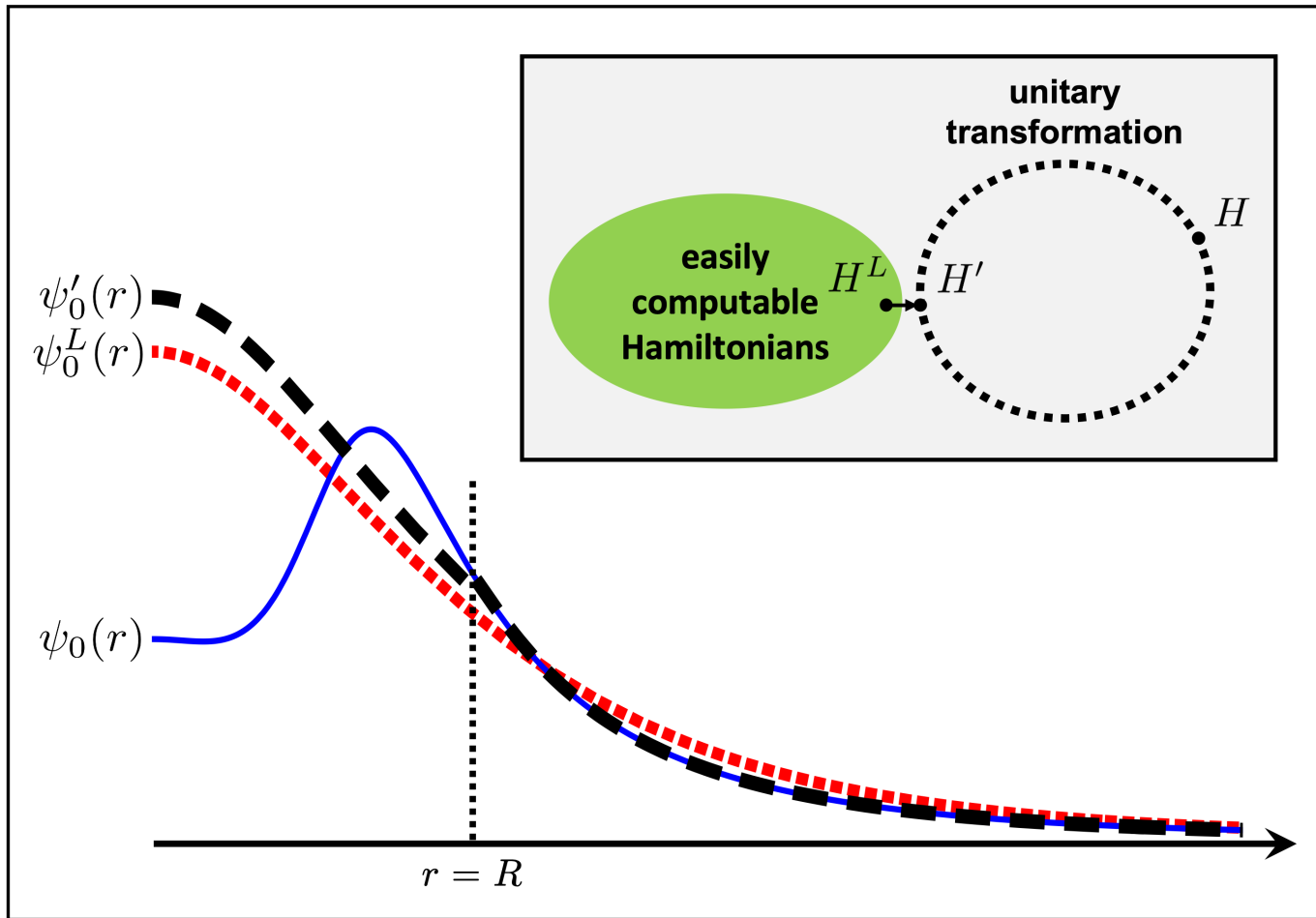
Shen, Elhatisari, Lähde, D.L., Lu, Meißner, Nature Commun. 14, 2777 (2023)

## Seeing the structure of $^{10}\text{Be}$

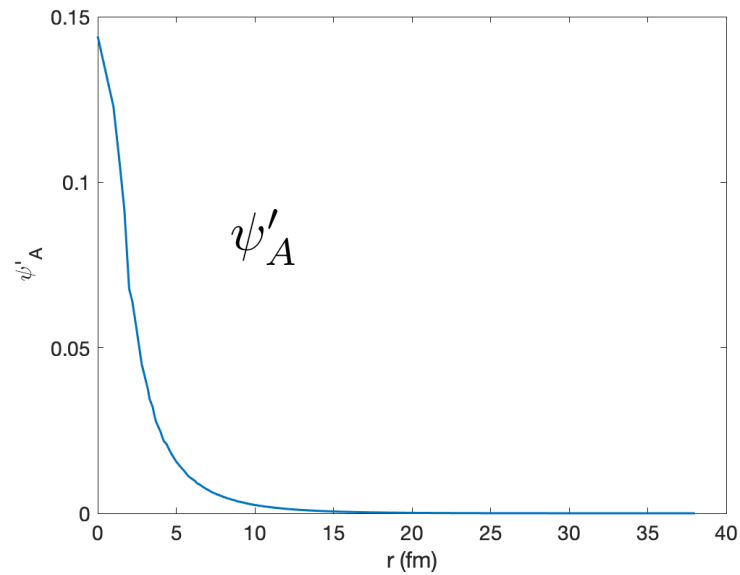
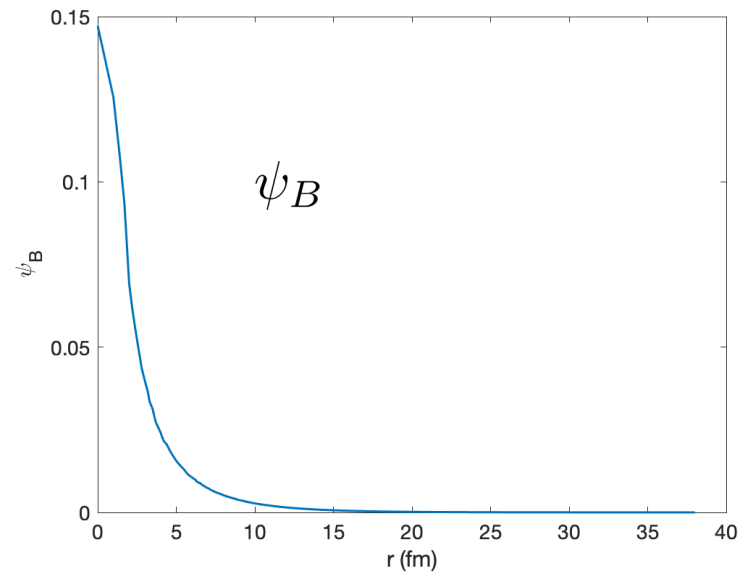
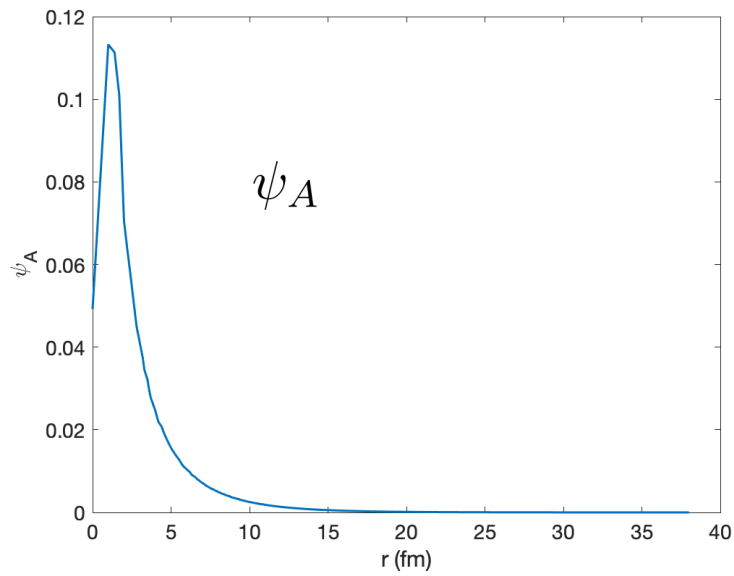


The left panel shows the intrinsic shape of the total nucleon density for  $^{10}\text{Be}$ . The right panel shows the density distribution of the two neutrons furthest away from the protons in  $^{10}\text{Be}$

# Wave function matching



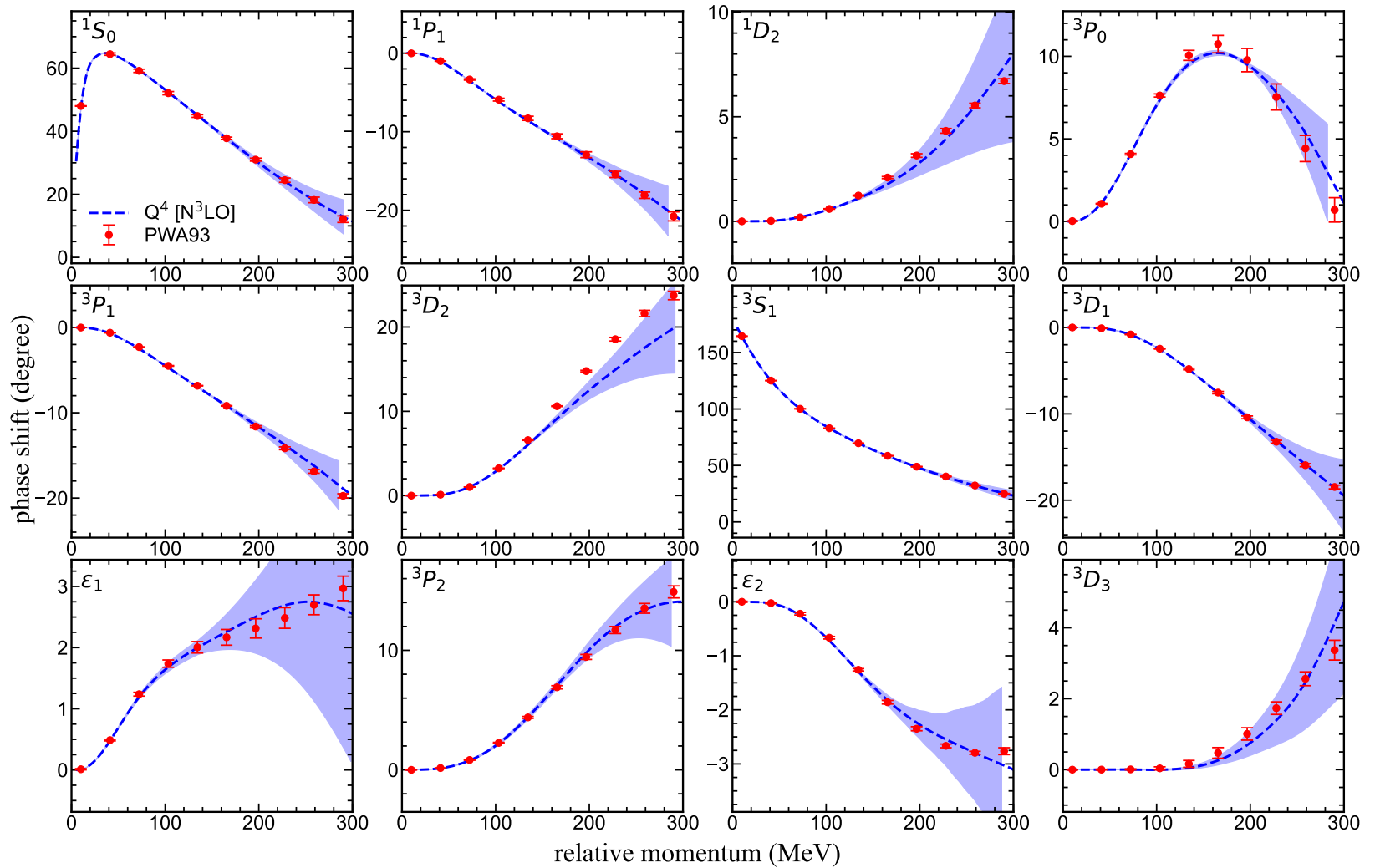
## Ground state wave functions



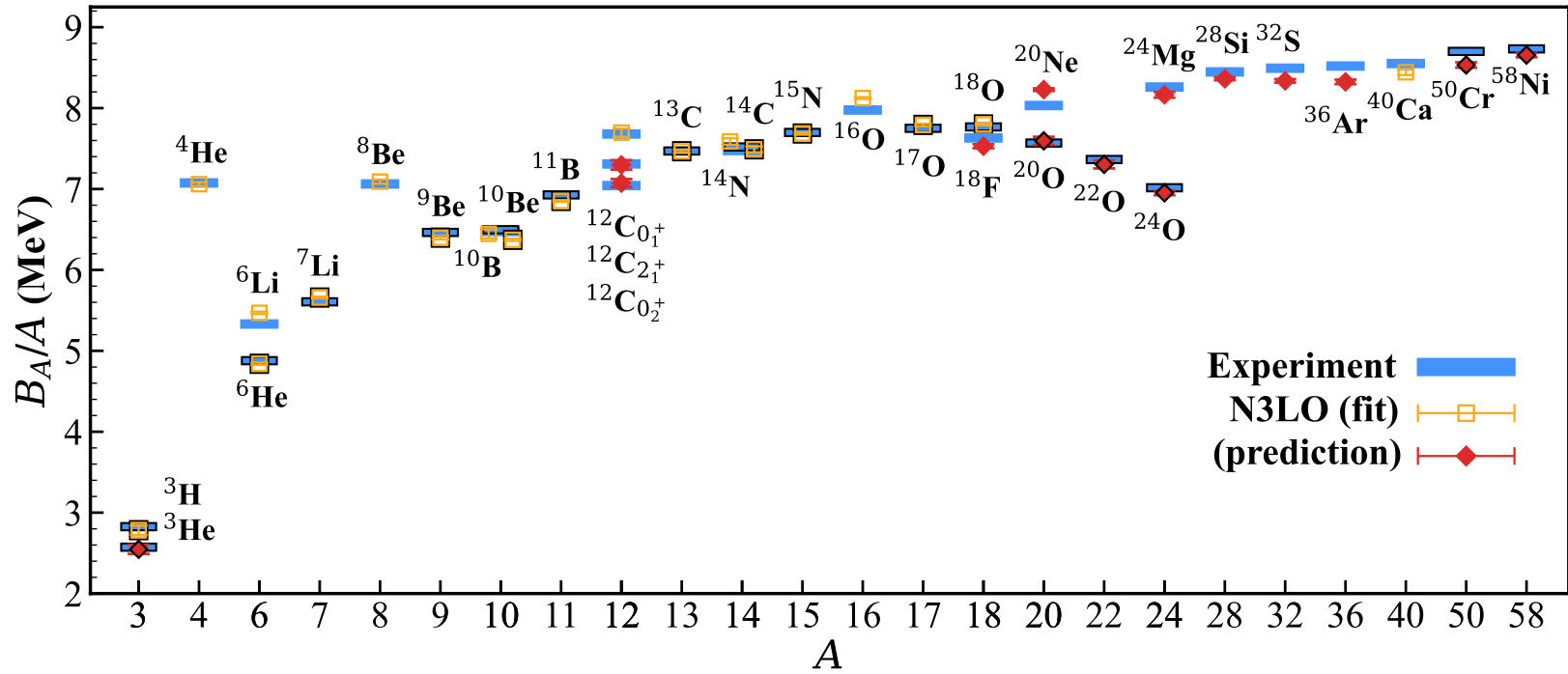
With wave function matching, we can now compute the eigenenergies starting from the eigenfunctions of  $H_B$  and using first-order perturbation theory.

$R = 2.6 \text{ fm}$		
$E_{A,n} = E'_{A,n} \text{ (MeV)}$	$\langle \psi_{B,n}   H_A   \psi_{B,n} \rangle \text{ (MeV)}$	$\langle \psi_{B,n}   H'_A   \psi_{B,n} \rangle \text{ (MeV)}$
-1.2186	3.0088	-1.1597
0.2196	0.3289	0.2212
0.8523	1.1275	0.8577
1.8610	2.2528	1.8719
3.2279	3.6991	3.2477
4.9454	5.4786	4.9798
7.0104	7.5996	7.0680
9.4208	10.0674	9.5137
12.1721	12.8799	12.3163
15.2669	16.0458	15.4840

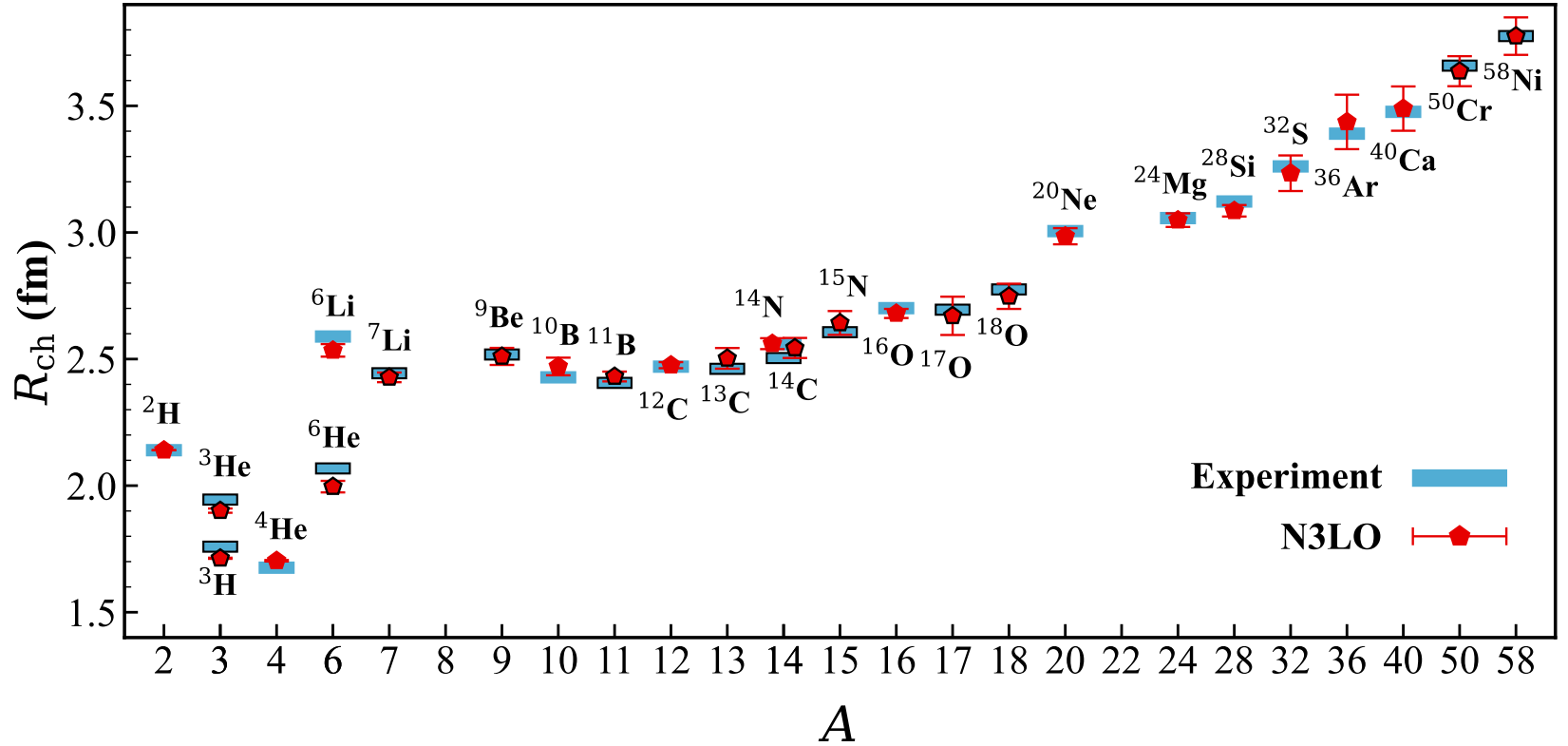
# N3LO chiral effective field theory interaction



## Binding energy per nucleon

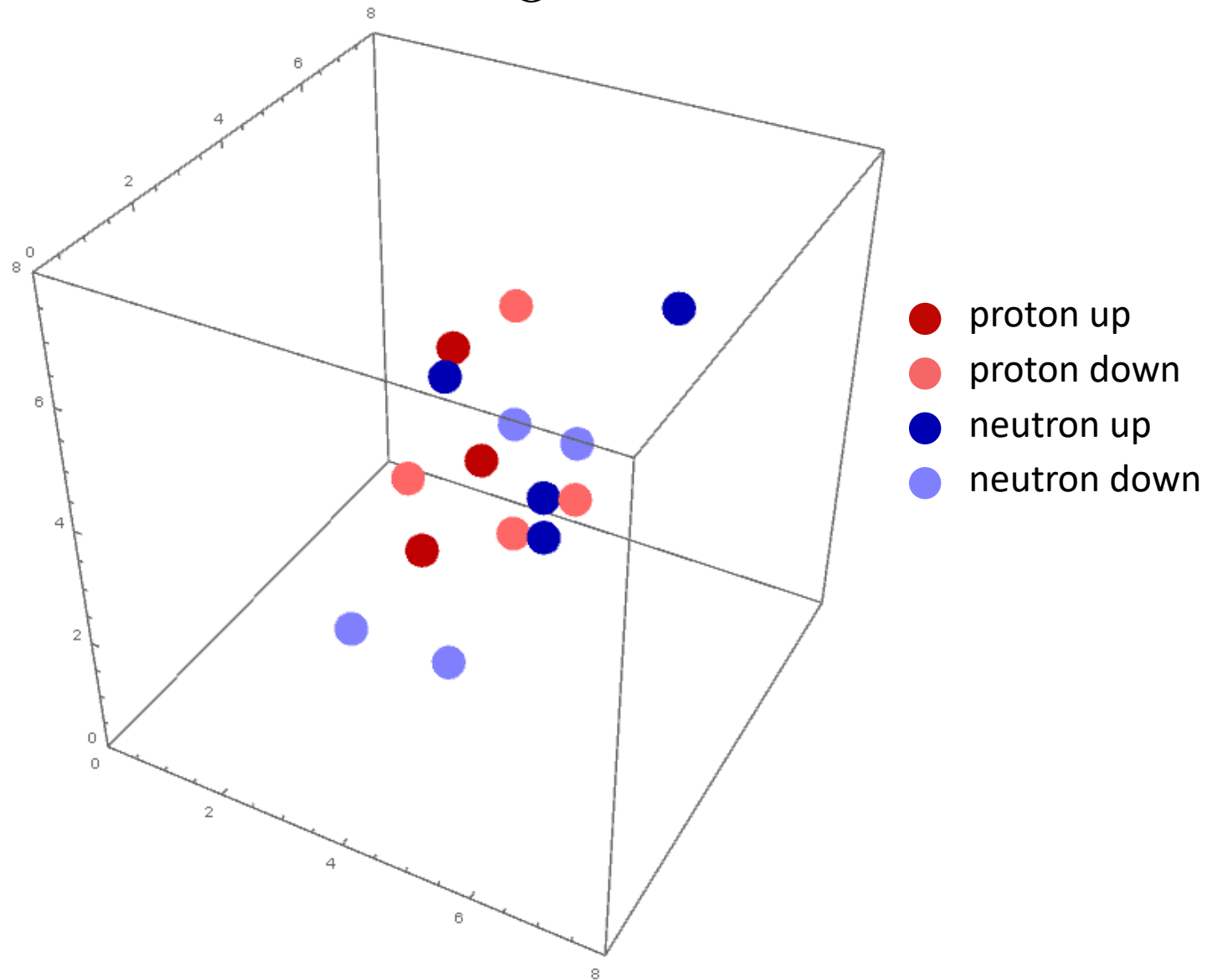


## Charge radius





$^{16}\text{O}$



## $^{16}\text{O}^{16}\text{O}$ collisions at RHIC and LHC energies

[Summerfield, Lu, Plumberg, D.L., Noronha-Hostler, Timmins PRC 104, L041901 (2021)]

$^{16}\text{O}^{16}\text{O}$  collisions have been proposed at RHIC and LHC to probe dependence on initial states of intermediate size, where alpha clustering is expected to be significant.

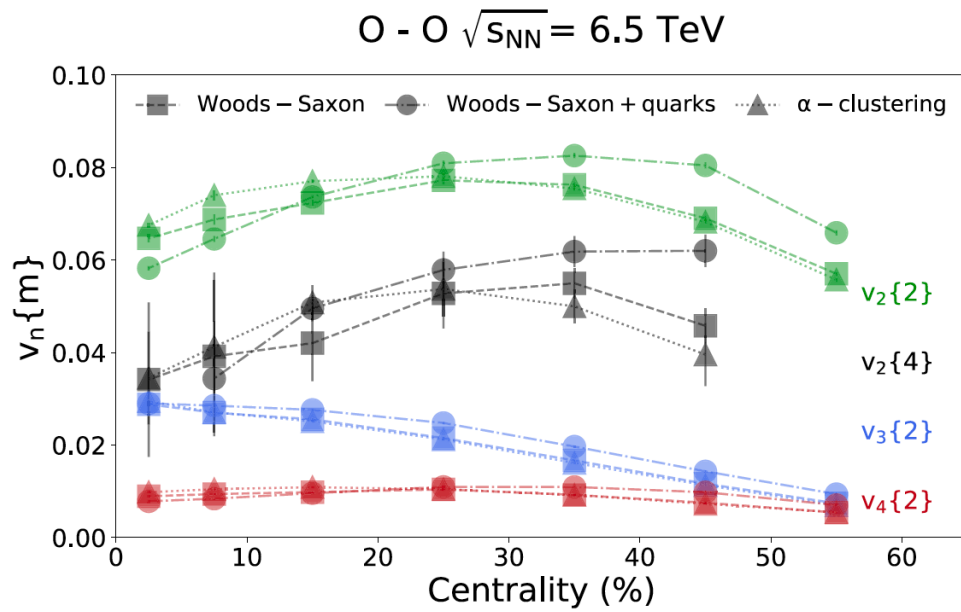
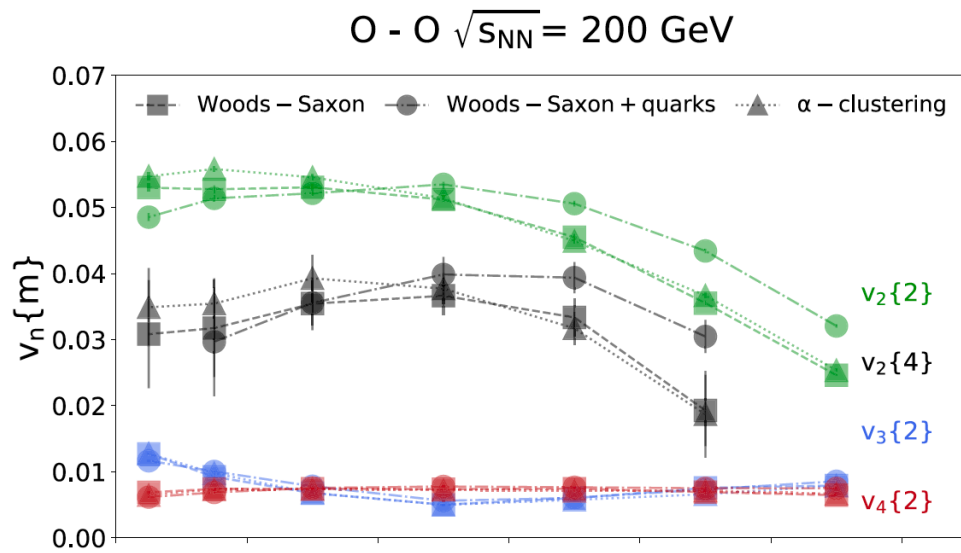
We use the T<sub>R</sub>ENTo model to general the initial entropy distribution.  
Moreland et al., Phys. Rev. C 92, 044903 (2015)

The initial entropy distribution is then passed through a free-streaming phase of duration 0.37 fm/*c* and used to initialize the hydrodynamics evolution.

We compute the following cumulants of the flow harmonics  $v_n$ :

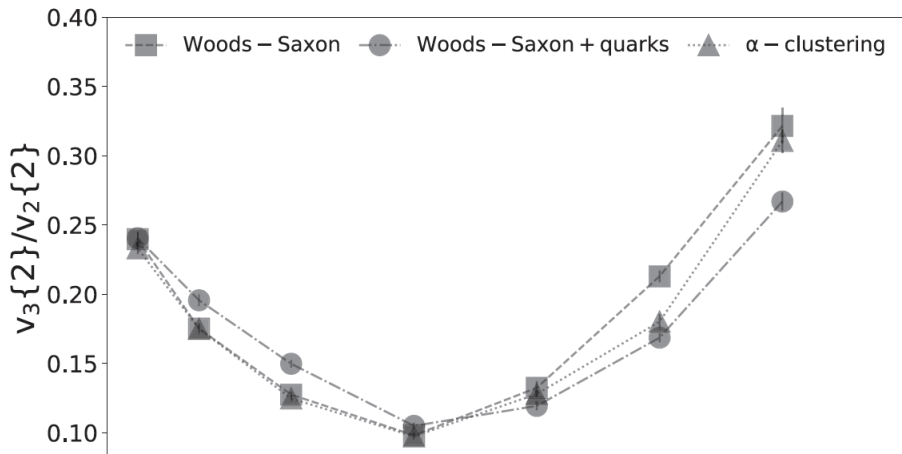
$$v_n\{2\} = [\langle v_n^2 \rangle]^{\frac{1}{2}}$$
$$v_n\{4\} = \left[ 2 \langle v_n^2 \rangle^2 - \langle v_n^4 \rangle \right]^{\frac{1}{4}}$$

We first compute results taking the initial density as a Woods-Saxon potential with density, radius, and diffusivity fitted to empirical values. We then consider the same Woods-Saxon potential, taking into account the quark substructure of the nucleons. Lastly, we consider using the nucleon distribution from the lattice effective field theory calculations. This will incorporate correlations such as alpha clustering.

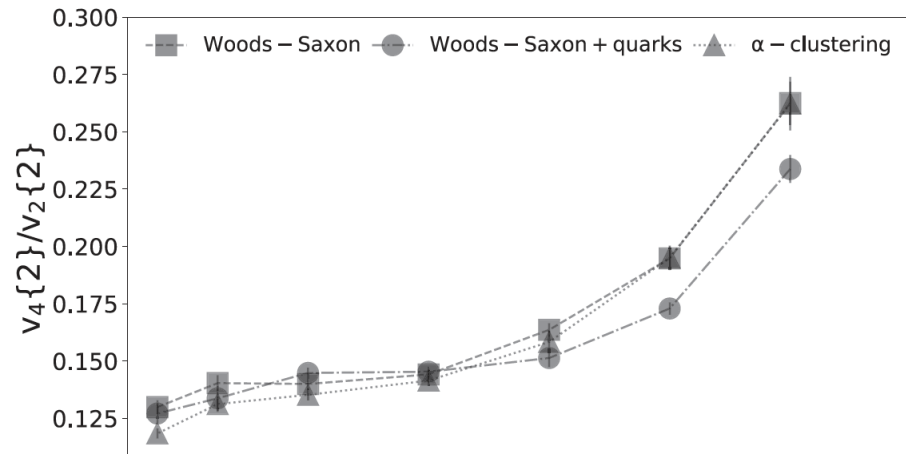


Summerfield, Lu, Plumberg, D.L., Noronha-Hostler, Timmins PRC 104, L041901 (2021)

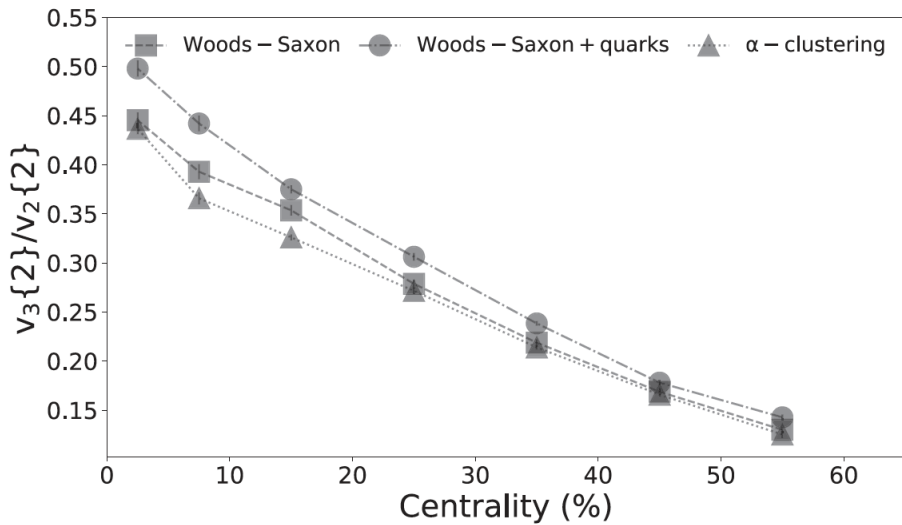
O - O  $\sqrt{s_{NN}} = 200$  GeV



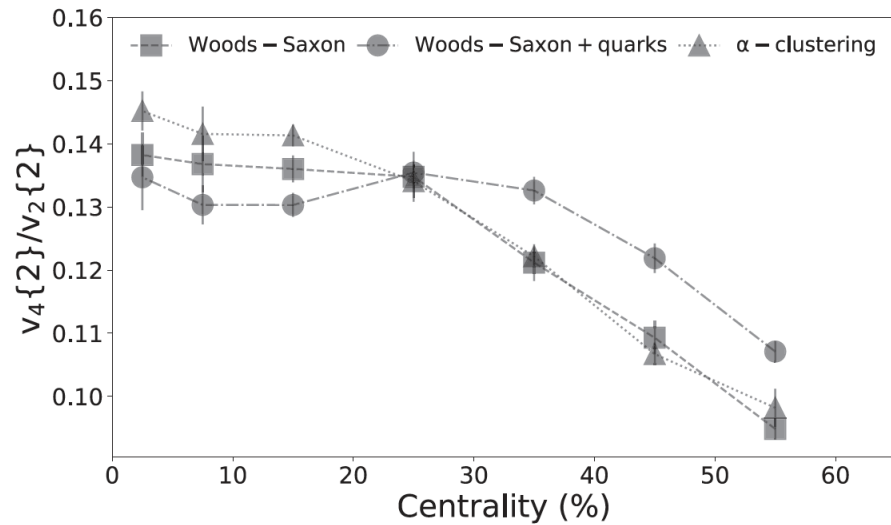
O - O  $\sqrt{s_{NN}} = 200$  GeV



O - O  $\sqrt{s_{NN}} = 6.5$  TeV



O - O  $\sqrt{s_{NN}} = 6.5$  TeV



Summerfield, Lu, Plumberg, D.L., Noronha-Hostler, Timmins PRC 104, L041901 (2021)

# STAR Collaboration Data for $^{16}\text{O}^{16}\text{O}$ collisions

S. Huang for the STAR Collaboration, arXiv:2312.12167

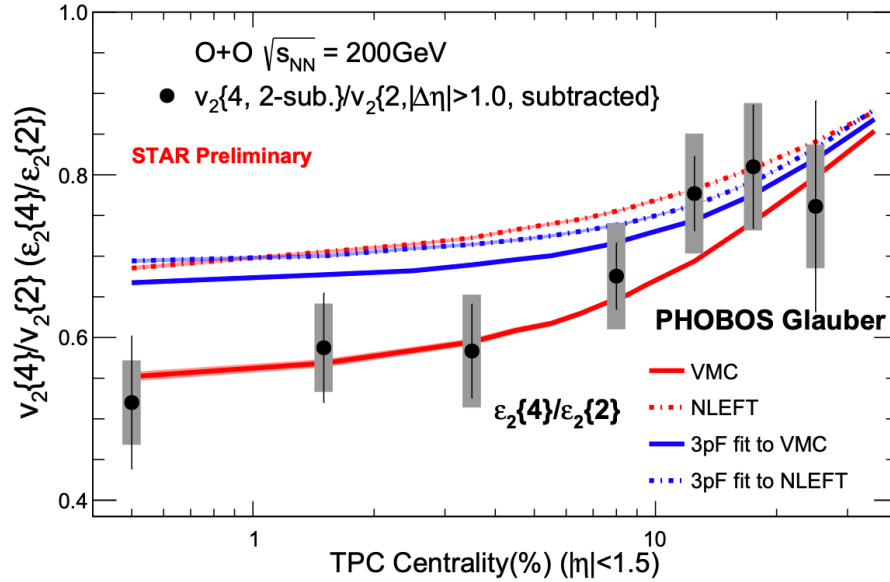


**Figure 3.** The figure illustrates  $v_2\{4\}/v_2\{2\}$  as a function of centrality, defined by charged hadron multiplicity at  $|\eta| < 1.5$ , in  $^{16}\text{O}+^{16}\text{O}$  collisions. Additionally, the  $\epsilon_2\{4\}/\epsilon_2\{2\}$  ratio from NLEFT, VMC, and two types of 3pF distributions are presented for comparison. Note that an issue is identified in the publicly available PHOBOS Glauber, which affected the implementation of the NLEFT and VMC configuration. This has been corrected in the updated figure

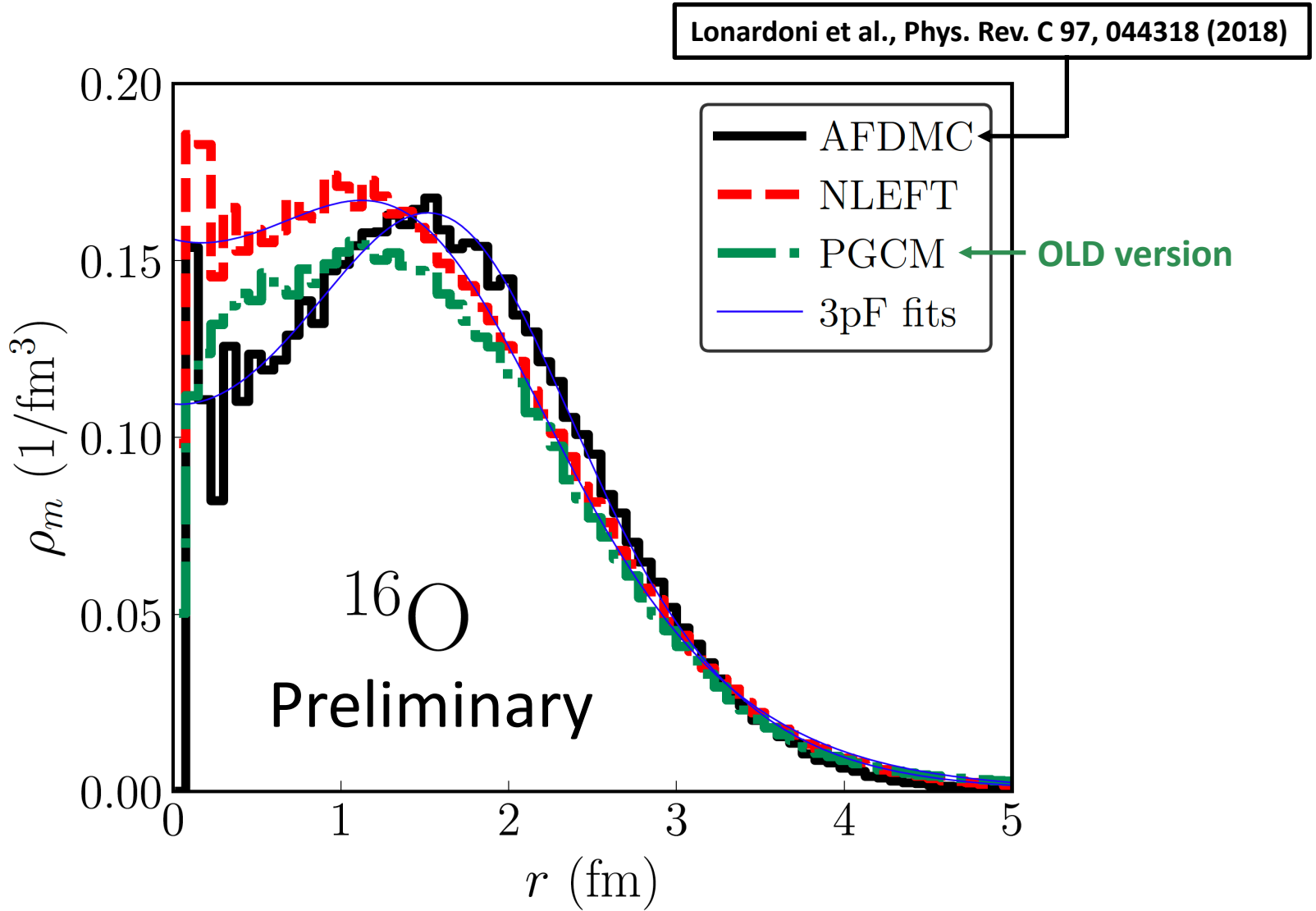


figure from Giuliano Giacalone

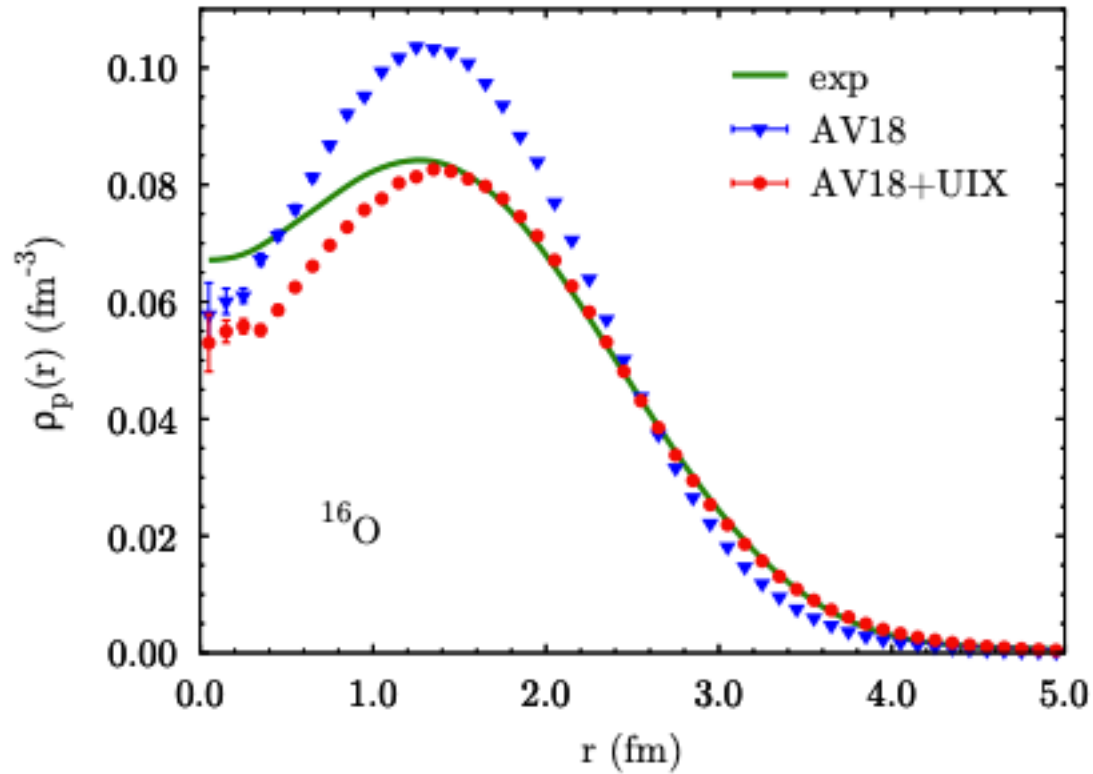


Figure 2. (Color online) Point proton densities in  $^{16}\text{O}$ . The green line refers to the “experimental” result, see text for details.



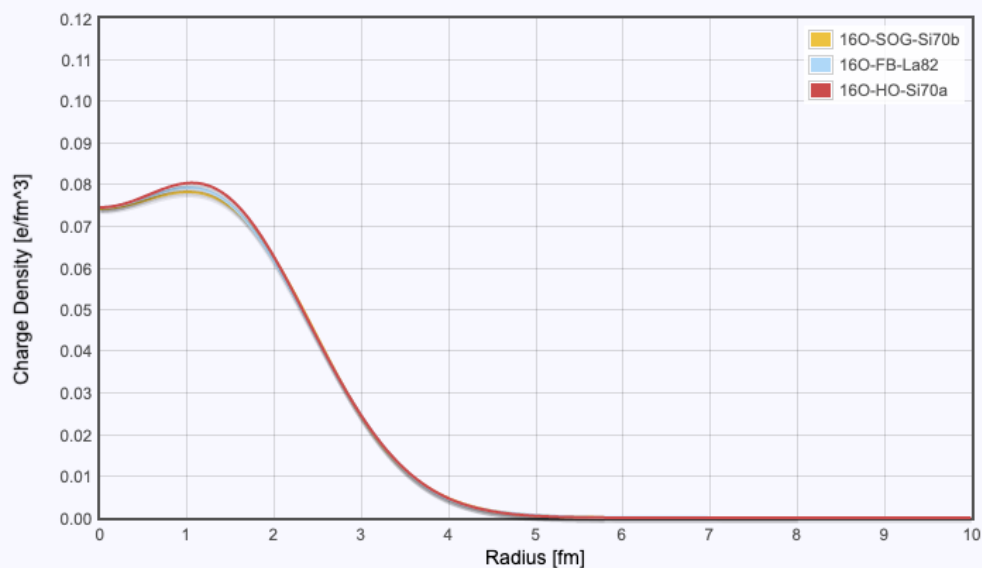
[Home](#) [Plot](#) [Download](#) [Charge Radii](#) [About](#)

## Nuclear Charge Density Archive - Plots

16O-SOG-Si70b

16O-FB-La82

16O-HO-Si70a



10

0.12

16O-SOG-Si70b

16O-FB-La82

16O-HO-Si70a

☐  $(A/Z) \cdot \rho(r)$

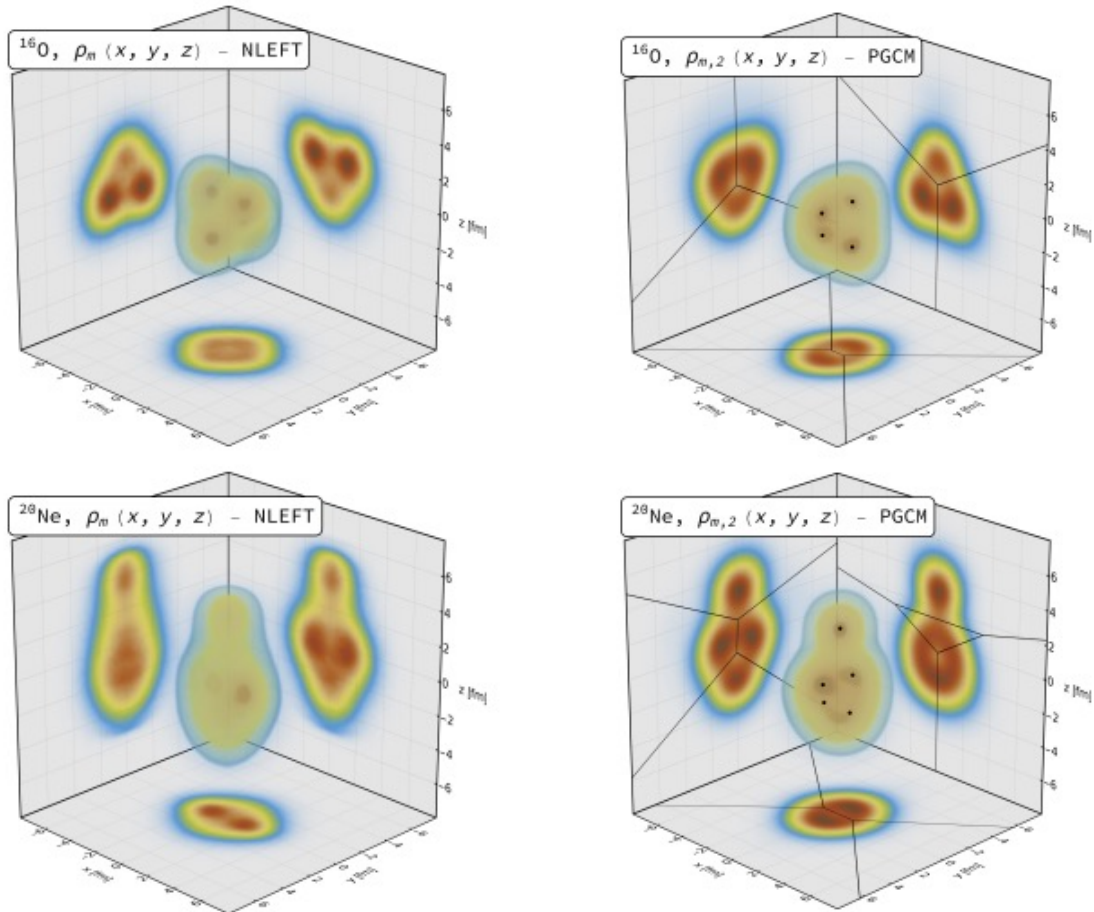
☒  $\rho(r)$

Select a nuclei from the drop-down box on the right. Then, select a normalization type using the radio buttons that appear (a radio button must be selected). Then click 'PLOT' to add the nuclei to the plot. To remove a plot, simply click the 'REMOVE' button next to the nuclei you would like to remove from the table on the left. To update the axes, use the sliders on the right side, then click 'PLOT' to update. To save an image of the graph, grab a screenshot of the page'

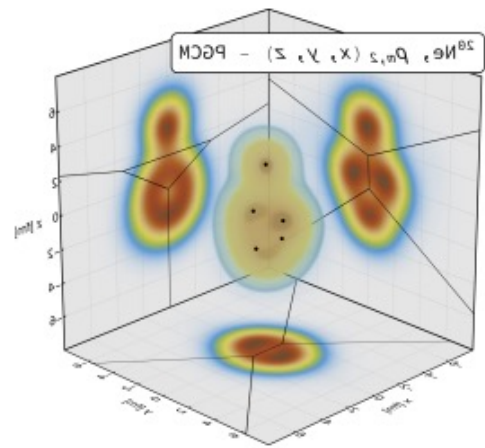
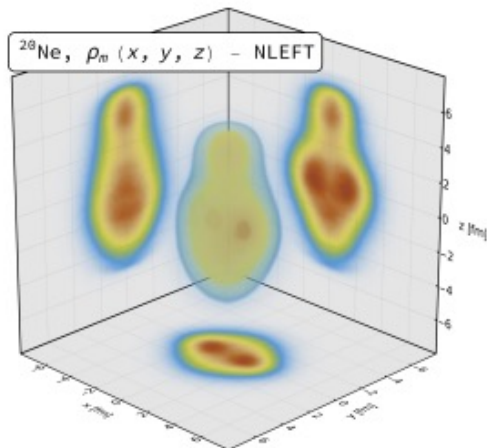
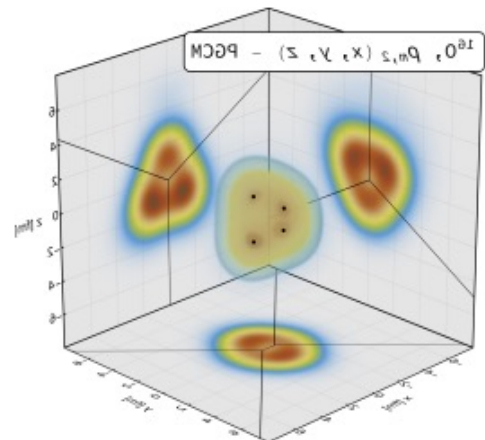
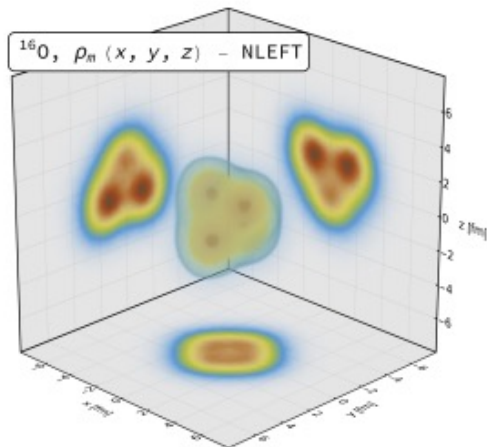
Note that 'non-normalized' ( $\rho(r)$ ) graphs do not have their plots scaled, whereas 'normalized' ( $(A/Z) \cdot \rho(r)$ ) graphs are scaled by a factor of  $(A/Z)$ .

Information about specific plot models can be found on the [About](#) page.

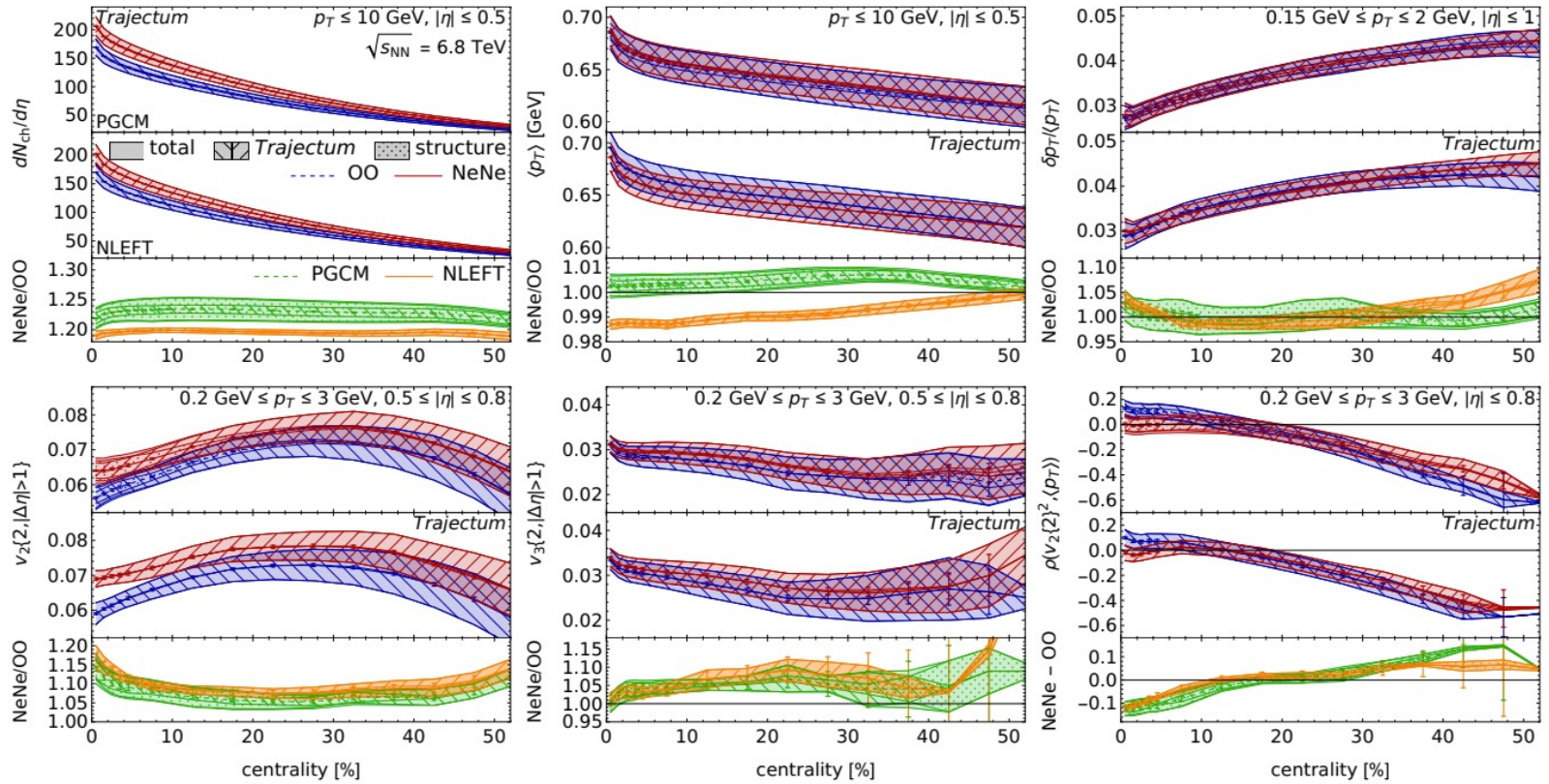
## $^{16}\text{O}^{16}\text{O}$ versus $^{20}\text{Ne}^{20}\text{Ne}$ collisions



Giacalone et al., arXiv:2402.05995



The elliptic flow of  $^{20}\text{Ne}^{20}\text{Ne}$  collisions is enhanced by as much as 1.170(8)stat.(30)syst. for NLEFT and 1.139(6)stat.(39)syst. for PGCM relative to  $^{16}\text{O}^{16}\text{O}$  collisions for the 1% most central events.



## Outlook

This talk started with an overview of different *ab initio* nuclear theory methods, including lattice EFT. It then described how lattice EFT is being used to predict nuclear structure. It also described how pinhole configurations provide *ab initio* data for initial states in relativistic heavy-ion collisions.

In a few years, it will be possible to do *ab initio* calculations of nuclear states across the nuclear chart using lattice EFT. We look forward to collaborating with our relativistic heavy-ion colleagues to explore this new field bringing together two different nuclear science communities.